POST PRINT

https://www.sciencedirect.com/science/article/abs/pii/S1388198116300245? via%3Dihub

https://doi.org/10.1016/j.bbalip.2016.02.003

Siculella L, Tocci R, Rochira A, Testini M, Gnoni A, Damiano F. Lipid accumulation stimulates the cap-independent translation of SREBP-1a mRNA by promoting hnRNP A1 binding to its 5'-UTR in a cellular model of hepatic steatosis. Biochim Biophys Acta. 2016 May;1861(5):471-81.

Highlights

1) Free fatty acids-induced lipid accumulation triggers HepG2 lipogenic genes expression

2) Proteolytic cleavage of SREBP-1a is stimulated in HepG2 cells treated with FFAs

3) FFAs promotes the nucleus-cytosolic shuttling of hnRNP A1 through the p38MAPK activation

4) FFAs induces hnRNP A1 binding to SREBP-1a mRNA, enhancing its translation.

5) HnRNP A1 silencing reduces FFAs-induced SREBP-1a expression and cell lipid accumulation

Lipid accumulation stimulates the cap-independent translation of SREBP-1a mRNA by promoting hnRNP A1 binding to its 5'-UTR in a cellular model of hepatic steatosis

Luisa Siculella[1*], Romina Tocci[1], Alessio Rochira[1], Mariangela Testini[1], Antonio Gnoni[2], Fabrizio Damiano[1]

[1] Laboratory of Biochemistry and Molecular Biology, Department of Biological and Environmental Sciences and Technologies, University of Salento, Lecce, Italy.

[2]Department of Basical Medical Sciences, Neurosciences, and Sensory Organs, University of Bari "Aldo Moro", Bari, Italy.

*Address correspondence to: Luisa Siculella, Laboratorio di Biochimica e Biologia Molecolare, Dipartimento di Scienze e Tecnologie Biologiche ed Ambientali, Università del Salento, Via Prov.le Lecce-Monteroni, Lecce 73100, Italy. E-mail: luisa.siculella@unisalento.it Telephone: +39-0832298696; Fax: +39-0832298626

Abstract

Non-alcoholic fatty liver disease (NAFLD) is a chronic disease characterized by accumulation of lipid droplets in hepatocytes. Enhanced release of non-esterified fatty acids from adipose tissue accounts for a remarkable fraction of accumulated lipids. However, the *de novo* lipogenesis (DNL) is also implicated in the etiology of the NAFLD. Sterol Regulatory Element-Binding Protein 1 (SREBP-1) is a transcription factor modulating the expression of several lipogenic enzymes. In the present study, in order to investigate the effect of lipid droplets accumulation on DNL, we used a cellular model of steatosis represented by HepG2 cells cultured in a medium supplemented with free oleic and palmitic fatty acids (FFAs). We report that FFAs supplementation induces the expression of genes coding for enzymes involved in the DNL as well as for the transcription factor SREBP-1a. The SREBP-1a mRNA translation, dependent on an Internal Ribosome Entry Site (IRES), and the SREBP-1a proteolytic cleavage are activated by FFAs. Furthermore, FFAs treatment enhances the expression and the nucleus-cytosolic shuttling of hnRNP A1, a trans-activating factor of SREBP-1a IRES. The binding of hnRNP A1 to the SREBP-1a IRES is also increased upon FFAs supplementation. The relocation of hnRNP A1 and the consequent increase of SREBP-1a translation are dependent on the p38 MAPK signal pathway, which is activated by FFAs. By RNA interference approach, we demonstrate that hnRNP A1 is implicated in the FFAs-induced expression of SREBP-1a and of its target genes as well as in the lipid accumulation in cells.

Keywords: Acetyl-CoA Carboxylase; Cap-independent translation; Lipid droplets; Non-alcoholic fatty liver disease; Sterol Regulatory Element-Binding Protein 1; Fatty Acid Synthase.

1. Introduction

Non-alcoholic fatty liver disease (NAFLD) is a chronic pathology in which accumulation of lipids in hepatocytes accounts for more than 5% of liver wet weight [1-3]. NAFLD is frequently found in obese and diabetic individuals [1], and it ranges from simple steatosis to non-alcoholic steatohepatitis (NASH), which is characterized by an inflammatory process with hepatic injury. Patients with NASH have a much higher risk of clinically significant pathologies, such as progressive liver fibrosis, cirrhosis, and hepatocellular carcinoma [1-3].

In the fatty liver, triglycerides are stored as lipid droplets in the cytoplasm. Dietary chylomicron remnants and lipolysis from adipose tissue are important sources for intrahepatic lipids accumulation. However, in NAFLD, a relevant fraction of hepatic lipids derives from the *de novo* lipogenesis (DNL) [4]. The causative role of the DNL in the etiology of NAFLD has been suggested by different studies [5-8]. Enhanced expression of lipogenic genes has been found in steatotic liver [5,6]. Furthermore, the down-regulation of genes coding for acetyl-CoA carboxylase 1 and 2 significantly reduces hepatic malonyl-CoA concentrations, lowers hepatic lipids accumulation, and improves hepatic insulin sensitivity in high fat diet-fed rats [7].

Sterol Regulatory Element-Binding Protein 1 (SREBP-1) belongs to the SREBPs family of basic helix–loop–helix-leucine zipper (bHLH-LZ) transcription factors, and it is referred as the master transcription factor regulating the expression of lipogenic genes [9]. Two isoforms of SREBP-1 have been described, SREBP-1a and SREBP-1c, both encoded by the Srebf1 gene. In liver, SREBP-1c is considered the major mediator of the lipogenic action of insulin and its expression is strictly regulated in animals and in humans in response to diet and hormones [10-12]. Conversely, SREBP-1a is constitutively expressed at low levels in liver and in most tissues of adult animals, and it is the predominant isoform in most cultured cell lines. However, SREBP-1a is an activator more potent than SREBP-1c and it activates the expression of all SREBPs-responsive genes, including those mediating the synthesis of fatty acids, triglycerides and cholesterol [12]. An enhanced expression of SREBP-1c has been observed in NAFLD [13-15], highlighting the role of this transcription factor in the lipid accumulation in fatty liver.

The disruption of endoplasmic reticulum (ER) homeostasis, known as ER stress, and the consequent activation of Unfolded Protein Response (UPR) are involved in both the development of NAFLD and its progression to NASH [16-21]. Interestingly, the expression and proteolytic cleavage of SREBP-1, as well as its transcriptional activity are increased in ER stressed cells [22-24].

NAFLD has been observed in patients with insulin resistance and hyperinsulinemia [25]. While the insulin increases the synthesis and the proteolytic processing of SREBP-1c in liver [26], the mechanism by which SREBP-1c is activated in liver, upon insulin resistance condition, is still object

of debate [27]. Moreover, deletion of SREBP-1c gene only partially reduces liver fat in *ob*/*ob* mice [28], suggesting that other SREBP isoforms besides SREBP-1c can be involved in NAFLD. Therefore, the implication of SREBP-1 in the NAFLD is not fully clarified.

The molecular mechanisms involved in the development of hepatic steatosis and its progression to chronic liver disease have been investigated in several animal models [29,30]. Isolated hepatocytes have been shown very useful to investigate the biochemical effects of lipid droplets accumulation when liver cells are cultured in a medium supplemented with different amounts of free palmitic (C16:0) and oleic (C18:1) acids (FFAs) [31-35]. These are the most abundant fatty acids in liver triglycerides in both healthy subjects and patients with NAFLD [36]. Primary culture of human hepatocytes is the model closest to human liver [31]; however, the scarcity of liver samples greatly hinders their use. An alternative model is the human hepatocyte-derived cell line HepG2 [31].

In the present study, we sought to deepen the molecular bases of the SREBP-1a activation in a cellular model of steatosis. Our results showed that FFAs supplementation induced the expression of genes coding for the transcription factor SREBP-1a, for the lipogenic enzymes acetyl-CoA carboxylase (ACACA) and fatty acid synthase (FASN), as well as for citrate carrier (CiC), a mitochondrial protein involved in DNL. Upon FFAs treatment, the proteolytic cleavage of SREBP-1a was also activated. Besides the activation of both UPR and the p38 MAPK signalling pathways, FFAs treatment led to an increase of the expression and the nucleus-cytosolic shuttling of the ribonucleoprotein hnRNP A1, which is a trans-activating factor of internal ribosome entry site (IRES). Upon FFAs supplementation, the binding of hnRNP A1 to the SREBP-1a 5' untranslated region (5'-UTR) increased as well, causing in turn an increment in the cap-independent translation of SREBP-1a.

2. Materials and methods

2.1 Plasmid construction

Plasmid pRS1aF was constructed by inserting the cDNA of SREBP-1a 5'-UTR (GenBank™ accession number NM001005291, 1-194) into the intercistronic site of the pRF vector [23]. Plasmids pRc-mycF (formerly pGL3utrH), and pREF (formerly pCREL), have been described previously [23,37]. PcDNA-SV5-hnRNPA1 was kindly provided by Ronald T. Hay (Wellcome Biocentre, University of Dundee) [38]. The plasmid containing the hnRNP A1 promoter inserted upstream the luciferase gene was kindly provided by James L. Manley (Department of Biological Sciences, Columbia University) [39].

2.2 Cell culture and transient transfection assay

HepG2 were maintained in DMEM (Dulbecco's modified Eagle's medium) 4500 mg/L glucose (D5796, Sigma) supplemented with 10% (v/v) heat-inactivated FBS (fetal bovine serum), penicillin

G (100 units/ml) and streptomycin (100 µg/ml). HepG2 cells were kept at 37°C in a humidified atmosphere containing 5% CO_2. In order to induce lipid accumulation in cells, a mixture of oleate/ palmitate 2:1 was prepared by dissolving the fatty acids in fatty acid-free BSA [31]. The molar ratio of fatty acids to albumin was 4:1. The albumin bound fatty acids were added to the culture medium at the final concentration of 0.25 mM, 0.5 mM, and 1.0 mM.

For transient transfections, 3.5×10^4 cells were seeded into 12-well plates 48 h before transfection. Cells were transfected using Metafectene Pro (Biontex Laboratories, Germany) following the manufacturer's instructions. After a transfection period of 8 h, the medium was changed to fresh DMEM supplemented with 10% (v/v) FBS and the cells were incubated for 24 h. After cells lysis, *Renilla* luciferase (RL) and firefly luciferase (FL) activities were measured using the Dual Luciferase Reporter Assay System (Promega). The β-galactosidase activity was determined using a β-galactosidase assay.

2.3 Extraction and quantification of triglycerides

Triglycerides content was assessed by spectrophotometric analysis by using a kit (Liqui Triglycerides, Futura System) that allows to quantify glycerol as a measure of triglycerides extracted by chloroform-methanol mixture 1:2 (v/v). Values were normalized for the protein amount and the data are expressed as percent of the triglycerides content relative to the control.

2.4 Isolation of RNA from cultured cells and real-time qPCR analysis

Total RNA from HepG2 cells was isolated using the SV Total RNA Isolation System kit (Promega), following the manufacturer's instructions. The RT (reverse transcriptase) reaction (20 µl) was carried out using 5 µg of total RNA, 100 ng of random hexamers and 200 units of SuperScript™ III RNase H-Reverse transcriptase (Life Technologies). Quantitative gene expression analysis was performed using SYBR® Select Master Mix for CFX (Life Technologies) and 18S rRNA for normalization. The primers used for real-time PCR analysis were as follows (5' to 3'): hCiCfor GAAGTTCATCCACGACCAGAC; hCiCrev TCGGTACCAGTTGCGCAGG; hFASNfor GAAGGAGGGTGTGTTTGCC; hFASNrev GGATAGAGGTGCTGAGCC; hACACAfor GCAACCAAGTAGTGAGGATG; hACACArev CTGTTTGGATGAGATGTGGG; hSREBP-1For ACACCATGGGGAAGCACAC; hSREBP-1Rev CTTCACTCTCAATGCGCC; hnRNPA1For AAGGGGCTTTGCCTTTGTAACCTT, hnRNPA1Rev CATTATAGCCATCCCCACTGCC; INSIG-1for ATCGTTCCAGAAGTGGCCTTG; INSIG-1rev ; INSIG-2for ATGTGACGCTCTTTCCACCTG, INSIG-2rev CACCGCATTACACTGGACCAC; SCAPfor GAGGTGCTGCCACCACAG; SCAPrev AGCCCATGGTTGTAGAAGGC; S1Pfor GTGATTGGAGTAGGCGGCAT; S1Prev TGGAGAAGCAACACTGGTCC; S2Pfor GGCTGGAAAACAACGGACTG; S2Prev GGCAATTACGCCAAACACCA.

2.5 Preparation of nuclear and cytosolic protein fractions from HepG2 cells and Western blot analysis

Nuclear and cytosolic protein fractions from HepG2 cells were prepared as previously described [40]. Briefly, HepG2 from 25 cm^2 flasks were pooled and centrifuged at 900 *g* for 5 min at 4°C. The resulting cell pellet was resuspended in Buffer 1 (Tris/HCl-pH 8.0 20 mM, NaCl 420 mM, EDTA 2 mM, Na_3VO_4 2 mM, Nonidet P-40 0.2%, glycerol 10%). Cells were passed several times through a 20 gauge syringe needle and then sonicated until no cells remained intact. The homogenate was centrifuged at 1,100 *g* for 10 min, and the surnatant was collected. The nuclear pellet was washed once in buffer 1 and then resuspended in Buffer 2 (Tris/HCl-pH 7.9 20 mM, NaCl 420 mM, KCl 10 mM, Na_3VO_4 0.1 mM, EDTA 1 mM, EGTA 1 mM, glycerol 20%). This suspension was rotated for 30 min and then centrifuged at 15,000 *g* for 30 min. The resulting surnatant is designated as the nuclear extract fraction. Protein concentration was determined using the Bio-Rad protein assay kit (Milan, Italy). 50 μg proteins were dissolved in sodium dodecyl sulfate (SDS) sample buffer and separated on 10% (w/v) SDS gels. Separated proteins were transferred electrophoretically onto nitrocellulose membrane (Pall, East Hills, NY). Equal protein loading was confirmed by Ponceau S staining. The filter was blocked with 5% (w/v) non-fat dried milk in buffered saline. Blots were incubated with specific primary antibodies directed against XBP1, (sc-7160), GRP78 (sc-13968), hnRNP A1 (sc-32301), SREBP-1 (sc-13551), p-ERK1/2 (sc-7383), p-p38 MAPKα (sc-17852-R) Insig-1 (SC-25124), Insig-2 (SC-34821), SCAP (SC-9675), S1P (sc-20757), S2P (sc-10863, Santa Cruz Biotechnology). The immune complexes were detected using appropriate peroxidase-conjugated secondary antibodies and enhanced chemiluminescent detection reagent (Pierce™ ECL Plus Western Blotting Substrate). Densitometric analysis was carried out on the Western-blots using the NIH Image 1.62 software (National Institutes of Health, Bethesda, MD), normalizing to β-Actin (sc-47778, Santa Cruz Biotechnology) or Lamin B (sc-6216, Santa Cruz Biotechnology) used as controls. In order to evaluate the effect of FFAs treatment on the hnRNP A1 degradation dependent on ubiquitin–26S proteasome system, HepG2 cells were incubated with 20 μM MG-132 for 1 h, followed by 0.5 mM FFAs or BSA.

2.6 pSREBP-1a and nSREBP-1a half life analysis

HepG2 cells were plated at a density of 1×10^6 cells into 25 cm^2 flask and incubated for 48 h. Cells were incubated for further 24 h in either the vehicle BSA- (control) or FFAs-supplemented medium. 100 μg/ml cycloheximide, inhibitor of protein synthesis, was added into the medium and cells were incubated for the indicated times. The half life of precursor (pSREBP-1) and the nuclear (nSREBP-1) form of SREBP-1 was also evaluated in the presence of 10 μg/ml cholesterol and 1 μg/ml 25-hydroxycholesterol which block the proteolytic cleavage of pSREBP-1a [41]. Sterols were added into

the medium five minutes prior the addition of cycloheximide. Then, cells were harvested and the level of pSREBP-1 and nSREBP-1 was analysed by Western blotting. The log of pSREBP-1a and nSREBP-1a content was reported as a function of time.

2.7 RNA Affinity Chromatography

DNA templates for synthesis of biotin-labelled RNA probes corresponding to the SREBP-1a and Encephalomyocarditis virus (EMCV) 5'-UTR were generated by PCR using as a template pRS1aF and pREF, respectively, and the following primers: SREBP-1a forward 5'-CGGCCGGGGGAACCCAGTT-3', SREBP-1a reverse 5'-CATGGCGCAGCCGCCTCCTC-3', EMCV forward 5'-CGTTACTGGCCGAAGCCG-3', EMCV reverse 5'-CCATGGTATTATCATCGTG-3'. All forward primers have anchored in the 5'-region of the T7 promoter sequence 5'-CGGAATTAATACGACTCACTATAGGG-3'. The biotin-labelled RNA probes were synthesized by T7 RNA polymerase (MAXIScript T7 RNA polymerase kit; Ambion) in the presence of Biotin-16-UTP, according to the manufacturer's protocol.

500 µg of cytosolic proteins from untreated (control) and FFAs-treated HepG2 cells were precleared by incubating with 300 µl Streptavidin MagneSphere® Paramagnetic Particles (Promega) for 1 h in 1 ml of Binding Buffer (Hepes/KOH-pH 7.9 20 mM, KCl 150 mM, Glycerol 5% (v/v), DTT 1mM, EDTA 0.5 mM, tRNA 25 µg/ml, PMSF 1.5mM, $MgCl_2$ 1.5mM). Precleared proteins were then incubated with 30 µg of SREBP-1a 5'-UTR biotin-RNA for 2 h. The EMCV 5'-UTR biotin-RNA was used as a negative control. 300 µl of paramagnetic particles were then added to the biotinylated RNA-protein complexes and incubated for 1 h. All incubations were performed at 4°C in constant rotation. The proteins retained on the paramagnetic particles were eluted in 50 µl of SDS-PAGE sample buffer at 95 °C for 2 min, separated by 10% (w/v) SDS-PAGE. The hnRNP A1 protein level was analysed by Western blot analysis by using the anti-hnRNP A1 monoclonal antibody.

2.8 RNA interference analysis

HnRNP A1 and *MAPK14* (*p38α MAPK*) gene silencing in HepG2 cells was performed by RNA interference with synthetic siRNA (*Silencer* ® Select Pre-designed siRNA, Ambion-Life Tecnologies; FlexiTube siRNA, Qiagen) directed at the sequences within the 3'-UTR region. A siRNA with a scrambled sequence was used as a negative targeting control. Transfection was performed by using HiPerFect Transfection Reagent (Qiagen) for 48 hours, according to the manufacturer's recommendations. The expression of hnRNP A1 was rescued by co-transfecting HepG2 cells with hnRNP A1-directed siRNA together with pcDNA-SV5-hnRNPA1. Transfection with pcDNA-SV5-hnRNPA1, which contains the hnRNP A1 ORF without its 3'-UTR, overrides the gene downregulation determined by hnRNP A1-specific siRNA, achieving the phenotypic rescue as a means of validating the hnRNP A1 function. To evaluate the effect of FFAs on SREBP-1a IRES

activity, HepG2 cells were co-transfected with the bicistronic pRS1aF construct together with either hnRNP A1-specific siRNA or scrambled siRNA for 48 h. After this period, hnRNP A1-knockdown cells and scrambled siRNA-transfected cells were incubated with FFAs for further 6 h. Then, cells were harvested and RL and FL activities were measured as described above.

2.9 Statistical analysis

Data represent means ± standard deviation (S.D.) of 4–5 replicates. Statistical analysis was carried out using the ANOVA test. The post hoc tests (Bonferroni/Dunn) were also performed. A *P*-value less than 0.05 was considered to achieve statistical significance.

3. Results

3.1 Fatty acids supplementation triggers the expression of SREBP-1a and of its target genes

Accumulation of lipid droplets was observed in HepG2 cells treated with 0.25 mM, 0.5 mM and 1.0 mM of FFAs for various times, as confirmed by microscopy after staining cells with Oil red O (ORO) (data not shown). Upon the FFAs supplementation, lipid content increased in a dose- and time-dependent manner, reaching the maximum level at 24 h (Fig. 1A). Conversely, no change in the lipid content was observed in the vehicle-incubated cells (data not shown). Treatment with 0.25 mM and 0.5 mM FFAs did not affect cell viability at all the times analysed (Fig. 1B), whereas a reduction of cell viability was observed in cells incubated with FFAs 1 mM at 12h and 24h (Fig. 1B). Therefore, the concentration of 0.5 mM was used in the subsequent experiments.

Treatment of HepG2 cells with 0.5 mM FFAs led to an increase of SREBP-1a mRNA level, reaching the maximum value (~2.5 fold vs control) at 12 h of treatment (Fig. 2A). The same treated cells showed a strong increment in the content of both the precursor (pSREBP-1a) and the nuclear (nSREBP-1a) form of SREBP-1a, rising up to a maximum level at 24 h (Fig. 2B). No significant changes in the SREBP-1a mRNA and protein contents were observed in control cells incubated with BSA alone (Supplementary Fig. 1).

To investigate whether FFAs treatment enhances protein stability, the half-life of pSREBP-1a and nSREBP-1a was determined in control (BSA) and in FFAs-treated cells. Results show an increase in the turnover of pSREBP-1a in FFAs-treated cells with respect to control cells (~2.7 h in FFAs-treated cells vs ~6.5 h in control cells) (Fig. 2C, left panel). The apparent half life of nSREBP-1a in FFAs-treated cells was similar to that in control cells (~5.7 h in FFAs-treated cells vs ~6.5 h in control cells) (Fig. 2C, left panel). The turnover of pSREBP-1a and nSREBP-1a was also evaluated in the presence of 10 μg/ml cholesterol and 1 μg/ml 25-hydroxycholesterol which block the proteolytic cleavage of pSREBP-1a [41]. In this condition, the half life of nSREBP-1a strongly diminished in FFAs-treated cells when compared to control cells (1.8 h in FFAs-treated cells vs 4.8 h in control cells). By contrast,

the decay curve of pSREBP-1a was similar in control cells and in FFAs-treated cells (Fig. 2C, right panel).

The SREBP-1 transactivation of lipogenic genes such as acetyl-CoA carboxylase (ACACA), fatty acid synthase (FASN) and mitochondrial citrate carrier (CiC) was evaluated by measuring the abundance of the corresponding mRNA. A time-dependent increase of ACACA, FASN and CiC mRNAs abundance was observed in cells upon FFAs supplementation to the culture medium (Fig. 2D).

3.2 Effect of fatty acids supplementation on SREBP-1a IRES activity

In a previous study, we identified an Internal Ribosome Entry Site (IRES) in the leader region of SREBP-1a mRNA, which mediates its cap-independent translation [23]. It has been also demonstrated that SREBP-1a IRES activity was induced by ER stress [14]. Here, we evaluated whether FFAs treatment was able to induce ER stress in the cells. To this aim, the content of Glucose-Regulated Protein 78 (GRP78), and X-box Binding Protein 1 (XBP1), two key markers of ER-stress, was analysed by Western blot analysis. FFAs treatment determines a time-dependent increment in the level of GRP78 and of the active form of XBP1 with respect to untreated cells (Supplementary Fig. 2A).

In order to evaluate the effect of FFAs treatment on the activity of SREBP-1a IRES, HepG2 cells were transfected with the bicistronic construct pRS1aF [23], which contains the human SREBP-1a 5'-UTR inserted between two reporter genes coding for the *Renilla* luciferase (RL) and firefly luciferase (FL), respectively (Fig. 3, upper panel) [23]. After transcription in cells, pRS1aF generates a bicistronic mRNA whose first cistron RL is translated via a cap-dependent mechanism, whereas the second cistron FL is translated independently on the cap structure, through the IRES of SREBP-1a 5'-UTR [23]. Transfection experiments were also performed by using pRc-mycF and pREF bicistronic constructs, containing the c-*myc* and EMCV 5'-UTR, respectively, located upstream the FL cistron (Fig. 3, upper panel). The treatment of HepG2 cells with FFAs increased the IRES activity of SREBP-1a mRNA by about 6-fold at 6 h compared to the untreated control cells (Fig. 3B, lower panel). FFAs caused an increase of c-*myc* IRES activity, reaching the maximum value (about 2-fold) at 12 h (Fig. 3, lower panel). By contrast, the IRES activity of EMCV 5'-UTR showed no significant changes. In all the experiments RL activity was reduced by the treatment with FFAs.

3.3 Effect of fatty acids on the binding of hnRNP A1 to SREBP-1a IRES

Previous findings showed that the efficiency of SREBP-1a mRNA translation is augmented upon the binding of hnRNP A1 to the SREBP-1a IRES [14]. The results reported in Fig. 4A showed that hnRNP A1 levels in the nuclei of FFAs-treated cells decreased after 3 h of FFAs treatment, reaching the minimum level at 24 h. On the other hand, a time-dependent increase in the cytosolic counterpart

of hnRNP A1 was observed upon FFAs treatment. It is known that the content of hnRNP A1 protein is regulated by the ubiquitin–26S proteasome system [42]. In the presence of 20 μM MG-132, an inhibitor of the ubiquitin–26S proteasome system, the effect of 0.5 mM FFAs addition on the increase of cytosolic hnRNP A1 content, and on the reduction of the nuclear fraction counterpart was stronger (Fig. 4B).

On these bases, we hypothesized that hnRNP A1 degradation triggered by FFAs treatment was counteracted by an increased expression of hnRNP A1. Quantitative real time PCR analysis showed indeed a time-dependent increase of hnRNP A1 mRNA upon FFAs addition to the medium (Fig. 4C). The promoter activity of hnRNP A1 gene is also increased in a time-dependent manner in FFAs-treated cells with respect to control cells (Fig. 4.D).

Then, we evaluated whether in FFAs-treated HepG2 cells the nucleus-cytosolic shuttling of hnRNP A1 could play a role in the activation of cap-independent translation of SREBP-1a, through the IRES activity. To test this hypothesis, the amount of hnRNP A1 bound to the SREBP-1a IRES in control and in cells with ER stress, induced by FFAs treatment, was analysed by RNA affinity chromatography. The results showed that the amount of cytosolic hnRNP A1 bound to the SREBP-1a probe was higher in FFAs-treated cells with respect to control cells (Fig. 4E, lanes 3 and 4). In contrast, hnRNP A1 was not detected when the EMCV RNA probe was used (Fig. 4E, lanes 1 and 2).

3.4 FFAs effects on SREBP-1a and on hnRNP A1 expression: implication of the p38 MAPK and Akt pathways

It has been demonstrated that the expression and the activity of SREBP-1 are under the control of MAPK/ERK, PI3K/Akt and p38 MAPK signal transduction pathways [43-45]. In order to evaluate the involvement of these signal pathways in the activation of SREBP-1a by FFAs, the time-dependent phosphorylation of ERK, Akt and p38 MAPK was analysed in HepG2 cells supplemented with 0.5 mM FFAs. The phosphorylation of P38 MAPK and, to a lesser extent, of Akt was strongly induced in FFAs-treated HepG2 cells. Minimal activation of ERK was also observed in the same conditions (Fig. 5A).

We hypothesized that the activation of signal pathways by FFAs could induce the shuttling from nuclei to cytosol of hnRNP A1 and, in turn, the cap-independent translation of SREBP-1a mRNA. To evaluate this hypothesis, the protein level of the cytosolic hnRNP A1 and those of pSREBP-1a and nSREBP-1a were analysed in control (BSA vehicle) and in FFAs-treated cells, in the presence or in the absence of a specific inhibitor of each kinase. In FFAs-treated cells, 25 μM LY294002, inhibitor of Akt, caused a slight increase of the pSREBP-1a, whereas nSREBP-1a was consistently reduced as compared to the corresponding levels observed in cells treated with FFAs alone. Conversely, the

content of cytosolic hnRNP A1 was unmodified by LY294002 in the presence of 0.5 mM FFAs (Fig. 5B). Interestingly, the incubation of FFAs-treated cells with 10 μM SB203580, a p38 MAPK specific inhibitor, caused a reduction of cytosolic hnRNP A1 and of both pSREBP-1a and nSREBP-1a with respect to FFAs-treated cells (Fig. 5B). The simultaneous treatment with LY294002 and SB203580 determined a reduction of pSREBP-1a and nSREBP-1a levels, reaching values lower than those observed in BSA-incubated cells (Fig. 5B). Experiments were also carried out using 30 μM PD98059, a MEK specific inhibitor; no significant changes in pSREBP-1a and nSREBP-1a as well as in hnRNP A1 levels were observed in FFA-treated cells (Fig. 5B). In the absence of FFAs, all the kinase inhibitors did not affect hnRNP A1, pSREBP-1a and nSREBP-1a contents (Fig. 5B).

The involvement of p38 MAPK in the FFAs-mediated increment of cytosolic hnRNP A1 content was also evaluated by RNA interference experiments. We found that the levels of cytosolic hnRNP A1 as well as of pSREBP-1a and nSREBP-1a increased in FFAs-treated cells transfected with scramble siRNA compared to the control cells. This increment was not observed upon transfection of FFAs-treated cells with p38 MAPK siRNA (Fig. 5C).

3.5 Effect of overexpression or knockdown of hnRNP A1 on the FFAs-mediated stimulation of SREBP-1a expression

In order to elucidate the role of hnRNP A1 in the SREBP-1a IRES activation by FFAs, a loss of function approach by RNA interference was used. The FFAs treatment strongly enhanced SREBP-1a protein levels in HepG2 cells transfected with scrambled siRNA (Fig. 6A, lane 2), but not in those transfected with hnRNP A1 siRNA (Fig. 6A, lane 3) when compared to the corresponding control cells (Fig. 6A, lane 1). The SREBP-1a expression in hnRNP A1-knockdown cells, supplemented with FFAs, was rescued after hnRNP A1 overexpression (Fig. 6A, lane 4). The role of hnRNP A1 on the FFAs-mediated induction of SREBP-1a IRES activity was also analysed. As reported in Fig. 6B, SREBP-1a IRES activity was approximately 4-fold in scrambled siRNA-transfected cells treated with FFAs (Fig. 6B, lane 2) compared to the untreated cells (Fig. 6B, lane 1). By contrast, FFAs treatment did not cause significant changes in IRES activity of SREBP-1a mRNA in hnRNP A1-knockdown cells (Fig. 6B, lane 3). In the same cells the induction of the SREBP-1a IRES activity upon FFAs treatment was rescued after overexpression of hnRNP A1 (Fig. 6B, lane 4).

The amount of mRNA for CiC, FASN and ACACA, whose genes are targets of SREBP-1 [9-12], was analysed by RT-qPCR under the same experimental conditions. The results reported in the Fig. 6C showed that the content of these mRNAs changed with a trend similar to that observed for SREBP-1a protein level (Fig. 6A). We then evaluated the effect of hnRNP A1 down-regulation on the lipid accumulation in FFAs-treated cells. The FFAs treatment increased the lipid content in HepG2 cells transfected with scrambled siRNA (Fig. 6D, lane 2). Interestingly, when the expression of hnRNP A1

was reduced, FFAs treatment caused an accumulation of lipids to a lesser extent than that observed in FFAs-treated cells transfected with scrambled siRNA (Fig. 6D, lane 3). The increase in the lipid content in hnRNP A1-knockdown cells, supplemented with FFAs, was rescued after the hnRNP A1 overexpression (Fig. 6D, lane 4).

3.6 FFAs effects on the expression of genes involved in the proteolytic cleavage of SREBP-1a

We analyzed the effect of FFAs treatment on the expression of SCAP, Insig-1, Insig-2, Site 1 protease, and Site 2 protease, which are involved in the proteolytic cleavage of SREBP-1. While the expression of Insig-2 and Site 2 protease did not show any change after FFAs-treatment, the mRNA abundance and the protein content of SCAP and Site 1 protease were induced by FFAs. The abundance of the Insig-1 mRNA increased in a time dependent manner upon addition of FFAs to the medium, whereas the content of the corresponding protein was reduced (Fig. 7).

4. Discussion

Non-alcoholic fatty liver disease (NAFLD), a syndrome affecting both adults and children, is characterized by fatty infiltration of the liver cells in the absence of chronic alcohol consumption or viral infection. Accumulated fatty acids in liver are mainly derived from adipose tissue lipolysis and from dietary chylomicron remnants. A substantial part of lipid accumulation derives from the DNL that contributes consistently to the hepatic steatosis [4,46,47]. The continuous activation of lipogenic pathway in the steatotic liver despite the large availability of intracellular lipids represents an intriguing paradox.

Given the wide and increasing incidence of NAFLD in the world population [48,49], numerous studies have been performed on this issue. However, the molecular mechanisms underlying the activation of lipogenic gene expression in hepatic steatosis remain poorly understood. SREBPs are transcription factors involved in the regulation of genes coding for the key enzymes of the fatty acids, triglycerides as well as cholesterol syntheses [9]. Several studies have demonstrated a close correlation between SREBP-1 expression and NAFLD [14,50,51].

Cellular models of hepatic steatosis have been developed in several works by incubating primary hepatocytes or hepatocyte-derived cell lines with different FFAs [31-35]. Even though these models cannot replace fatty liver, they are a useful tool to study steatosis *in vitro*. Incubation of hepatocytes with FFAs mixture containing 2:1 oleate/palmitate is frequently used since higher concentration of oleate counteracts the pro-apoptotic effects observed when palmitate alone is used [31,32,34]. To note that treatment of human hepatocytes or HepG2 cells with a mixture of oleate/palmitate 2:1 caused an intracellular lipid accumulation similar to that observed in steatotic liver [31]. In the present study, the experiments have been carried out in HepG2 cells incubated with oleate/palmitate 2:1, 0.2-0.5 mM, concentrations similar to those of plasmatic non esterified fatty acids (NEFA) measured in

patients with metabolic syndrome [34,52]. Thus, we used this model of hepatic steatosis to investigate the effect of lipid accumulation on SREBP-1 expression. Addition to HepG2 cells of FFAs up to 0.5 mM caused an increment of lipid content as well as of the SREBP-1 expression, without affecting cell viability (Fig. 1). Since SREBP-1a represents the predominant isoform expressed in cultured cell lines [41], the findings obtained in FFAs-stressed HepG2 cells led us to speculate that the change in SREBP-1 protein and mRNA content is likely to be referred to an increased expression of SREBP-1a, rather than of SREBP-1c.

The increase in the SREBP-1a content cannot be ascribed to an increment in protein stability (Fig. 2), since the turnover of SREBP-1a observed in FFAs-treated cells augmented. This finding could be related to the proteasome-mediated degradation of SREBP-1 as reported by [53]. The degradation process occurs through the phosphorylation of Ser and Thr residues in the C-terminus of both the active SREBP-1a and SREBP-1c by GSK-3β, followed by the ubiquitination through the ubiquitin ligase SCF^{Fbw7} [53]. Another mechanism affecting the SREBP-1 stability involves the phosphorylation of Thr-426 by stress-activated p38 MAPK, which reduces the SUMOylation of SREBP-1, and enhances its stability [54]. Here, we found that FFAs treatment strongly activates p38 MAPK (Fig. 5), without increasing the SREBP-1a stability. Further studies are required to clarify the polyubiquitination and/or SUMOylation in the FFAs-mediated degradation of SREBP-1a.

The release of mature and active SREBPs through the proteolytic cleavage of the precursor molecule is the main regulation mechanism governing their transcriptional activity [28]. The half life experiments showed that FFAs treatment induces the SREBP-1a proteolytic cleavage (Fig. 2). A depletion of Insig-1 protein level has been observed upon FFAs treatment, despite the increase of the corresponding mRNA. The FFAs-mediated effect on Insig-1 turnover, together with the increase of SCAP protein level (Fig. 7) could explain the induction of SREBP-1a processing by FFAs treatment. A disappearance of Insig-1 has been also described in fructose-fed mice and in ER-stressed CHO cells, where an enhanced proteolytic cleavage of SREBP-1c and of SREBP-2, respectively, was observed [55,56]. The reduction of Insig-1 has been justified by the general inhibition of protein synthesis occurring upon activation of UPR pathway [16,55]. Here, we demonstrated that FFAs treatment caused the induction of ER stress in HepG2 cells, as shown by the increased levels of GRP78 and XBP1 proteins, two key markers of UPR (Supplementary Fig. 2).

It has been shown that incubation of human embryonic kidney cells (HEK-293) with oleate alone reduced SREBP-1 expression and processing [57]. Conversely, in this study we observed that, upon addition of the mix oleate/palmitate 2:1 to HepG2 cells, both the expression and the proteolytic cleavage of SREBP-1a increased, through the induction of ER stress and the stress-responsive MAPK pathways. Similarly, an induction of SREBP-1 expression by the oleate/palmitate mix has been

observed in primary rat hepatocytes and in rat liver cell line BRL-3A [35]. Thus, the differences in cell lines used and in FFA treatments should be taken into account to explain the discrepancy of results.

In previous works, we found that ER stress enhances the cap-independent translation of SREBP-1a mRNA, through the involvement of an IRES, identified in the 5'-UTR [23,58]. The addition of 0.5 mM FFAs to the culture medium resulted in an increase of the SREBP-1a and c-Myc IRES activity. Vice versa, the IRES activity of EMCV was not significantly affected by the addition of FFAs (Fig. 3). The different response of SREBP-1a and c-Myc IRES activities compared to that of EMCV IRES can suggest a specificity of FFAs effect on different IRESs. In all cases, a reduction of the cap-dependent protein synthesis was observed in ER-stressed cells, as suggested by the reduction of *Renilla* luciferase activity. In a recent study it has been shown that hnRNP A1 is a IRES trans-activating factor (ITAF) interacting with the SREBP-1a IRES [14]. HnRNP A1 is a nucleo-cytoplasmic shuttling protein that regulates gene expression, acting on metabolism and translation of mRNA [59]. The cytoplasmic redistribution of hnRNP A1 has been observed during viral infection and cellular stress, such as osmotic shock or UVC irradiation [60-63]. The findings here reported showed that treatment with FFAs caused: (i) the nucleus-cytoplasmic shuttling of hnRNP A1, (ii) the induction of hnRNP A1 expression, (iii) the increase of the binding of hnRNP A1 to the SREBP-1a 5'-UTR (Fig. 4). HnRNP A1 shuttling is promoted by the activation of p38 MAPK-Mnk1/2 pathway [59-61]. Notably, p38 MAPK inhibition reduced the cytosolic hnRNP A1 level as well as both pSREBP-1a and nSREBP-1a protein level in FFAs-treated cells (Fig. 5). These data indicate that FFAs-induced ER stress stimulates the shuttling of hnRNP A1, which in turn activates the expression of the SREBP-1a, through the cap-independent translation of its mRNA. Conversely, Akt inhibition caused a reduction of the proteolytic cleavage of SREBP-1a as evidenced by the detected decrease of nSREBP-1a level and the concomitant, slight increase of pSREBP-1a (Fig. 5B). This result is consistent with the role of Akt in the SREBP-1 activation by proteolytic cleavage [64]. Indeed, it has been shown that Akt pathway is involved in the ER-to-Golgi transport of the complex SREBP-1 cleavage activating protein (SCAP)/pSREBP-1 [65]. The simultaneous inhibition of both p38 MAPK and Akt in FFAs-treated cells resulted in a strong decrease of SREBP-1a protein level which was lower than that observed in the FFAs-untreated control cells (Fig. 5B). It should be stressed that, even though the activation of SREBP-1a occurs through the proteolytic cleavage of its precursor protein, the enhanced translation of SREBP-1a, stimulated by the p38 MAPK pathway, is crucial in order to maintain high levels of both precursor and mature SREBP-1a, and to counteract their increased turnover rate in FFAs-treated cells. The critical role of hnRNP A1 in the FFAs-mediated activation of lipogenic genes expression has been elucidated by loss- and gain-of-function experiments. The

FFAs-mediated increase of the SREBP-1a IRES activity and of the expression of SREBP-1a and of its target genes (i.e. ACACA, FASN, and CiC), was dependent on the hnRNP A1 expression. Moreover, FFAs-mediated increment of lipid content was reduced in hnRNP A1-knockdown cells with respect to that observed in FFAs-treated cells transfected with scramble siRNA, whereas it was unchanged after hnRNP A1 overexpression (Fig. 6). CiC is a protein embedded in the inner mitochondrial membrane and plays an important role in the intermediary metabolism. CiC transports, in the form of citrate, acetyl-CoA from mitochondria to the cytosol. Cytosolic acetyl-CoA is the starter molecule for both DNL and cholesterol synthesis. Since SREBP-1a promotes the expression of genes involved in the synthesis of cholesterol, such as 3-hydroxy-3-methylglutaryl-Coenzyme A reductase (HMGCR) [22], the stimulation of SREBP-1a expression by FFAs could also have implications on cholesterol homeostasis. It has been reported an alternative splicing of HMGCR mRNA mediated by hnRNP A1, whose subcellular distribution is activated by the MKK3/6-p38MAPK signaling cascade [66].

An interesting question is whether translation of mRNA for SREBP-1c as well as for SREBP-2 could be incremented by FFAs-induced ER stress, through a mechanism similar to that described for SREBP-1a mRNA [14]. However, the presence of a cryptic promoter makes characterization of the SREBP-1c 5'-UTR difficult [14].

To our knowledge, this is the first study in which the involvement of hnRNP A1 in the induction of the human SREBP-1 expression in a cellular model of steatosis has been investigated, highlighting the molecular mechanism by which supplementation of FFAs causes the increment of the DNL. In this model, the FFAs-induced shuttling of hnRNP A1 enhances SREBP-1a translation, through the activation of p38 MAPK pathway. Further investigations *in vivo* can shed light on the implication of SREBP-1a regulation at translational level in metabolic disorders such as NAFLD.

ABBREVIATIONS

ACACA, Acetyl-CoA carboxylase alpha; EMCV, Encephalomyocarditis virus; CiC, Citrate carrier; ER, endoplasmic reticulum; FFAs, Free fatty acids; FASN, Fatty acid synthase; FL, Firefly luciferase; IRES, Internal ribosome entry site; NAFLD, Non-alcoholic fatty liver disease; ORF, open reading frame; RL, *Renilla* luciferase; SREBP-1, Sterol regulatory element-binding protein-1; UTR, untranslated region.

FUNDING

This study was supported by Grants from Apulia Region (Italy), PON 01_01958 PIVOLIO.

ACKNOWLEDGMENTS

We thank Dr Anne Willis (MRC Toxicology Unit, University of Leicester) for providing the pRc-mycF, Dr Ronald T. Hay (Wellcome Biocentre, University of Dundee) for pcDNA-SV5-hnRNPA1; Dr Matteo Serino and Dr Christian Touriol (Institut National de la Santé et de la Recherche Médicale, Toulose) for pCREL; Dr James L. Manley (Columbia University) for the construct containing the hnRNP A1 promoter in pGL3 plasmid.

REFERENCES

[1] G. Musso, R. Gambino, M. Cassader, G. Pagano, Meta-analysis: natural history of non-alcoholic fatty liver disease (NAFLD) and diagnostic accuracy of non-invasive tests for liver disease severity, Ann. Med. 43 (2011) 617–649.

[2] J.K. Dowman, J.W. Tomlinson, P.N. Newsome, Systematic review: the diagnosis and staging of non-alcoholic fatty liver disease and non-alcoholic steatohepatitis, Aliment Pharmacol. Ther. 33 (2011) 525–540.

[3] L.A. Adams, O.R. Waters, M.W. Knuiman, R.R. Elliott, J.K. Olynyk, NAFLD as a risk factor for the development of diabetes and the metabolic syndrome: an eleven-year follow-up study, Am. J. Gastroenterol. 104 (2009) 861–867.

[4] K.L. Donnelly, C.I. Smith, S.J. Schwarzenberg, J. Jessurun, M.D. Boldt, E.J. Parks, Sources of fatty acids stored in liver and secreted via lipoproteins in patients with nonalcoholic fatty liver disease, J. Clin. Invest. 115 (2005) 1343–1351.

[5] E. Lima-Cabello, M.V. García-Mediavilla, M.E. Miquilena-Colina, J. Vargas-Castrillón, T. Lozano-Rodríguez, M. Fernández-Bermejo, J.L. Olcoz, J. González-Gallego, C. García-Monzón, S. Sánchez-Campos, Enhanced expression of pro-inflammatory mediators and liver X-receptor-regulated lipogenic genes in non-alcoholic fatty liver disease and hepatitis C, Clin. Sci. 120 (2011) 239–250.

[6] A. Ferramosca, A. Conte, F. Damiano, L. Siculella, V. Zara, Differential effects of high-carbohydrate and high-fat diets on hepatic lipogenesis in rats. Eur. J. Nutr. 53 (2014) 1103–1114.

[7] D.B. Savage, C.S. Choi, V.T. Samuel, Z.X. Liu, D. Zhang, A. Wang, X.M. Zhang, G.W. Cline, X.X. Yu, J.G. Geisler, S. Bhanot, B.P. Monia, G.I. Shulman, Reversal of diet-induced hepatic steatosis and hepatic insulin resistance by antisense oligonucleotide inhibitors of acetyl-CoA carboxylases 1 and 2, J. Clin. Invest. 116 (2006) 817–824.

[8] M. Miyazaki, M.T. Flowers, H. Sampath, K. Chu, C. Otzelberger, X. Liu, J.M. Ntambi, Hepatic Stearoyl-CoA Desaturase-1 deficiency protects mice from carbohydrate-induced adiposity and hepatic steatosis, Cell Metab. 6 (2007) 484–496.

[9] W. Shao, P.J. Espenshade, Expanding roles for SREBP in metabolism, Cell Metab. 16 (2012) 414–419.

[10] P.J. Espenshade, A.L. Hughes, Regulation of sterol synthesis in eukaryotes, Annu. Rev. Genet. 41 (2007) 401–427.
[11] F. Damiano, E. Mercuri, E. Stanca, G.V. Gnoni, L. Siculella, Streptozotocin-induced diabetes affects in rat liver citrate carrier gene expression by transcriptional and posttranscriptional mechanisms, Int. J. Biochem. Cell Biol. 43 (2011) 1621–1629.
[12] T.I. Jeon, T.F. Osborne, SREBPs: metabolic integrators in physiology and metabolism, Trends Endocrinol. Metab. 23 (2012) 65–72.
[13] P. Ferré, F. Foufelle, Hepatic steatosis: a role for de novo lipogenesis and the transcription factor SREBP-1c, Diabetes Obes. Metab. 12, (2010) 83–92.
[14] F. Damiano, A. Rochira, R. Tocci, S. Alemanno, A. Gnoni, L. Siculella, HnRNP A1 mediates the activation of the IRES-dependent SREBP-1a mRNA translation in response to endoplasmic reticulum stress, Biochem. J. 449 (2013) 543–553.
[15] T. Horie, T. Nishino, O. Baba, Y. Kuwabara, T. Nakao, M. Nishiga, S. Usami, M. Izuhara, N. Sowa, N. Yahagi, H. Shimano, S. Matsumura, K. Inoue, H. Marusawa, T. Nakamura, K. Hasegawa, N. Kume, M. Yokode, T. Kita, T. Kimura, K. Ono, MicroRNA-33 regulates sterol regulatory element-binding protein 1 expression in mice, Nat. Commun. 4 (2013) 2883.
[16] C.L. Gentile, M. Frye, M.J. Pagliassotti , Endoplasmic reticulum stress and the unfolded protein response in nonalcoholic fatty liver disease, Antioxid. Redox Signal. 15 (2011) 505–521.
[17] S.M. Colgan, A.A. Hashimi, R.C. Austin, Endoplasmic reticulum stress and lipid dysregulation, Expert Rev. Mol. Med. 13 (2011) e4.
[18] A.H. Lee, E.F. Scapa, D.E. Cohen, L.H. Glimcher, Regulation of hepatic lipogenesis by the transcription factor XBP1, Science 320 (2008) 1492–1496.
[19] M. Flamment, H.L. Kammoun, I. Hainault, P. Ferré, F. Foufelle, Endoplasmic reticulum stress: a new actor in the development of hepatic steatosis, Curr. Opin. Lipidol. 21 (2010) 239–246.
[20] L. Dara, C. Ji, N. Kaplowitz, The contribution of endoplasmic reticulum stress to liver diseases, Hepatology 53 (2011) 1752–1763.
[21] S. Basseri, R.C. Austin, Endoplasmic reticulum stress and lipid metabolism: mechanisms and therapeutic potential, Biochem. Res. Int. 2012 (2012) 841362.
[22] G.H. Werstuck, S.R. Lentz, S. Dayal, G.S. Hossain, S.K. Sood, Y.Y. Shi, J. Zhou, N. Maeda, S.K. Krisans, M.R. Malinow, Austin RC, Homocysteine-induced endoplasmic reticulum stress causes dysregulation of the cholesterol and triglyceride biosynthetic pathways, J. Clin. Invest. 107 (2001) 1263–1273.

[23] F. Damiano, S. Alemanno, G.V. Gnoni, L. Siculella, Translational control of the sterol-regulatory transcription factor SREBP-1 mRNA in response to serum starvation or ER stress is mediated by an internal ribosome entry site, Biochem. J. 429 (2010) 603–612.

[24] H.L. Kammoun, H. Chabanon, I. Hainault, S. Luquet, C. Magnan, T. Koike, T. Koike, P. Ferré, F Foufelle, GRP78 expression inhibits insulin and ER stress-induced SREBP-1c activation and reduces hepatic steatosis in mice. J. Clin. Invest. 119 (2009) 1201–1215.

[25] K. Cusi, Role of obesity and lipotoxicity in the development of nonalcoholicsteatohepatitis: pathophysiology and clinical implications, Gastroenterology 142 (2012) 711–725.e6.

[26] I. Shimomura, Y. Bashmakov, S. Ikemoto, J.D. Horton, M.S. Brown, J.L. Goldstein, Insulin selectively increases SREBP-1c mRNA in the livers of rats with streptozotocin-induced diabetes, Proc. Natl. Acad. Sci. U.S.A. 96 (1999) 13656–13661.

[27] C. Postic, J. Girard, Contribution of de novo fatty acid synthesis to hepatic steatosis and insulin resistance: lessons from genetically engineered mice, J. Clin. Invest. 118 (2008) 829–838.

[28] Y.A. Moon, G. Liang, X. Xie, M. Frank-Kamenetsky, K. Fitzgerald, V. Koteliansky, M.S. Brown, J.L. Goldstein, J.D. Horton, The Scap/SREBP pathway is essential for developing diabetic fatty liver and carbohydrate-induced hypertriglyceridemia in animals, Cell Metab. 15 (2012) 240–246.

[29] A. Koteish, A.M. Diehl, Animal models of steatosis, Semin. Liver Dis. 21 (2001) 89–104.

[30] C.S. Lieber, Alcoholic fatty liver: its pathogenesis and mechanism of progression to inflammation and fibrosis, Alcohol 34 (2004) 9–19.

[31] M.J. Gómez-Lechón, M.T. Donato, A. Martínez-Romero, N. Jiménez, J.V. Castell, J.E. O'Connor, A human hepatocellular in vitro model to investigate steatosis, Chem. Biol. Interact. 165 (2007) 106–116.

[32] Ricci M, Odoardi MR, Carulli L, Anzivino C, Ballestri S, Pinetti A, Fantoni LI, Marra F, Bertolitti M, Banni S, Lenardo A, Carulli N, Loria P: Differential effect of oleic acid and palmitic acid on lipid accumulation and apoptosis in cultured hepatocytes. J. Gastroenterol. Hepatol. 24 (2009) 830–840.

[33] E. Grasselli, A. Voci, L. Canesi, R. De Matteis, F. Goglia, F. Cioffi, E. Fugassa, G Gallo, L. Vergani, Direct effects of iodothyronines on excess fat storage in rat hepatocytes. J. Hepatol. 54 (2011) 1230–1236.

[34] E. Grasselli, A. Voci, L. Canesi, A. Salis, G. Damonte, A.D. Compalati, F. Goglia, G. Gallo, L. Vergani, 3,5-diiodo-L-thyronine modifies the lipid droplet composition in a model of hepatosteatosis, Cell. Physiol. Biochem. 33 (2014) 344–356.

[35] Hassan W, Rongyin G, Daoud A, Ding L, Wang L, Liu J, Shang J. Reduced oxidative stress contributes to the lipid lowering effects of isoquercitrin in free fatty acids induced hepatocytes. Oxid. Med. Cell. Longev. 2014 (2014) 313602.

[36] J. Araya, R. Rodrigo, L.A. Videla, L. Thielemann, M. Orellana, P. Pettinelli, J. Poniachik, Increase in long-chain polyunsaturated fatty acid n−6/n−3 ratio in relation to hepatic steatosis in patients with non-alcoholic fatty liver disease, Clin. Sci. 106 (2004) 635–643.

[37] M. Stoneley, F.E. Paulin, J.P.C. Le Quesne, S.A. Chappell, A.E. Willis, c-Myc 5' untranslated region contains an internal ribosome entry segment, Oncogene 16 (1998) 423–428.

[38] D.C. Hay, G.D. Kemp, C. Dargemont, R.T. Hay, Interaction between hnRNP A1 and IκBα is required for maximal activation of NF-κB-dependent transcription, Mol. Cell. Biol. 21 (2001) 3482–3490.

[39] C.J. David, M. Chen, M. Assanah, P. Canoll, J.L. Manley, HnRNP proteins controlled by c-Myc deregulate pyruvate kinase mRNA splicing in cancer, Nature 463 (2010) 364–368.

[40] F. Damiano, R. Tocci, G.V. Gnoni, L. Siculella, Expression of citrate carrier gene is activated by ER stress effectors XBP1 and ATF6α, binding to an UPRE in its promoter, Biochim. Biophys. Acta 1849 (2015) 23–31.

[41] I. Shimomura, H. Shimano, J.D. Horton, J.L. Goldstein, M.S. Brown, Differential expression of exons 1a and 1c in mRNAs for sterol regulatory element binding protein-1 in human and mouse organs and cultured cells, J. Clin. Invest. 99, (1997) 838–845.

[42] A. Iervolino, G. Santilli, R. Trotta, C. Guerzoni, V. Cesi, A. Bergamaschi, C. Gambacorti-Passerini, B. Calabretta, D. Perrotti, HnRNP A1 nucleocytoplasmic shuttling activity is required for normal myelopoiesis and BCR/ABL leukemogenesis, Mol. Cell. Biol. 22 (2002) 2255–2266.

[43] G.V. Gnoni, A. Rochira, A. Leone, F. Damiano, S. Marsigliante, L. Siculella, 3,5,3'triiodo-L-thyronine induces SREBP-1 expression by non-genomic actions in human HEPG2 cells, J. Cell Physiol. 227 (2012) 2388–2397.

[44] J. Kotzka, B. Knebel, J. Haas, L. Kremer, S. Jacob, S. Hartwig, U. Nitzgen, D. Muller-Wieland, Preventing phosphorylation of sterol regulatory element-binding protein 1a by MAP-kinases protects mice from fatty liver and visceral obesity, PLoS One 7 (2012) e32609.

[45] A. Rochira, F. Damiano, S. Marsigliante, G.V. Gnoni, L. Siculella, 3,5-Diiodo-l-thyronine induces SREBP-1 proteolytic cleavage block and apoptosis in human hepatoma (Hepg2) cells, Biochim. Biophys. Acta 1831 (2013) 1679–1689.

[46] P. Priore, A. Cavallo, A. Gnoni, F. Damiano, G.V. Gnoni, L. Siculella, Modulation of hepatic lipid metabolism by olive oil and its phenols in nonalcoholic fatty liver disease, IUBMB Life 67 (2015) 9–17.

[47] J.E. Lambert, M.A. Ramos-Roman, J.D. Browning, E.J. Parks, Increased de novo lipogenesis is a distinct characteristic of individuals with nonalcoholic fatty liver disease, Gastroenterology 146 (2014) 726–735.

[48] M. Bertolotti, A. Lonardo, C. Mussi, E. Baldelli, E. Pellegrini, S. Ballestri, D. Romagnoli, P. Loria, Nonalcoholic fatty liver disease and aging: epidemiology to management, World J Gastroenterol. 20 (2014) 14185–14204.

[49] N. Rosso, N.C. Chavez-Tapia, C. Tiribelli, S. Bellentani, Translational approaches: from fatty liver to non-alcoholic steatohepatitis, World J. Gastroenterol. 20 (2014) 9038–9049.

[50] I. Shimomura, Y. Bashmakov, J.D. Horton, Increased levels of nuclear SREBP-1c associated with fatty livers in two mouse models of diabetes mellitus, J. Biol. Chem. 274 (1999) 30028–30032.

[51] J.C. Cohen, J.D. Horton, H.H. Hobbs, Human fatty liver disease: old questions and new insights, Science 332 (2011) 1519–1523.

[52] E. Ferrannini , E.J. Barrett, S. Bevilacqua, R.A. Fronzo, Effect of fatty acids on glucose production and utilization in man, J. Clin. Invest. 72 (1983) 1737–1747.

[53] M.T. Bengoechea-Alonso, J. Ericsson, A phosphorylation cascade controls the degradation of active SREBP1. J. Biol. Chem. 284 (2009) 5885–5895.

[54] M. Arito, T. Horiba, S. Hachimura, J. Inoue, R. Sato R, Growth factor-induced phosphorylation of sterol regulatory element-binding proteins inhibits sumoylation, thereby stimulating the expression of their target genes, low density lipoprotein uptake, and lipid synthesis. J. Biol. Chem. 283 (2008) 15224–15231.

[55] J.N. Lee, J. Ye, Proteolytic activation of sterol regulatory element-binding protein induced by cellular stress through depletion of Insig-1. J. Biol. Chem. 279 (2004) 45257–45265.

[56] C. Zhang, X. Chen, R.M. Zhu, Y. Zhang, T. Yu, H. Wang, H. Zhao, M. Zhao, Y.L. Ji, Y.H. Chen, X.H. Meng, W. Wei, D.X. Xu, Endoplasmic reticulum stress is involved in hepatic SREBP-1c activation and lipid accumulation in fructose-fed mice. Toxicol Lett. 212 (2012) 229–240.

[57] V.C. Hannah, J. Ou , A. Luong, J.L. Goldstein, M.S. Brown, Unsaturated fatty acids down-regulate srebp isoforms 1a and 1c by two mechanisms in HEK-293 cells. J. Biol. Chem. 276 (2001) 4365–4372.

[58] A.M. Giudetti, F. Damiano, G.V. Gnoni, L. Siculella, Low level of hydrogen peroxide induces lipid synthesis in BRL-3A cells through a CAP-independent SREBP-1a activation, Int. J. Biochem. Cell Biol. 45 (2013) 1419–1426.

[59] J. Jean-Philippe, S. Paz, M. Caputi, HnRNP A1: the Swiss army knife of gene expression, Int. J. Mol. Sci. 14 (2013) 18999–19024.

[60] W. van der Houven van Oordt, M.T. Diaz-Meco, J. Lozano, A.R. Krainer, J. Moscat, J.F. Cáceres, The MKK(3/6)-p38-signaling cascade alters the subcellular distribution of hnRNP A1 and modulates alternative splicing regulation, J. Cell Biol. 149 (2000) 307–316.
[61] E. Allemand, S. Guil, M. Myers, J. Moscat, J.F. Cáceres, A.R. Krainer, Regulation of heterogenous nuclear ribonucleoprotein A1 transport by phosphorylation in cells stressed by osmotic shock, Proc. Natl. Acad. Sci. U.S.A. 102 (2005) 3605–3610.
[62] S. Guil, J.C. Long, J.F. Cáceres, HnRNP A1 relocalization to the stress granules reflects a role in the stress response, Mol. Cell. Biol. 26 (2006) 5744–5758.
[63] A. Cammas, F. Pileur, S. Bonnal, S.M. Lewis, N. L´evêque, M. Holcik, S. Vagner, Cytoplasmic relocalization of heterogeneous nuclear ribonucleoprotein A1 controls translation initiation of specific mRNAs, Mol. Biol. Cell. 18 (2007) 5048–5059.
[64] T. Porstmann, B. Griffiths, Y.L. Chung, O. Delpuech, J.R. Griffiths, J. Downward, A. Schulze, PKB/Akt induces transcription of enzymes involved in cholesterol and fatty acid biosynthesis via activation of SREBP, Oncogene 24 (2005) 6465–6481.
[65] X. Du, I. Kristiana, J. Wong, A.J. Brown, Involvement of Akt in ER-to-Golgi transport of SCAP/SREBP: A link between a key cell proliferative pathway and membrane synthesis, Mol. Biol. Cell. 17 (2006) 2735–2745.
[66] C.Y. Yu, E. Theusch, K. Lo, L.M. Mangravite, D. Naidoo, M. Kutilova, M.W. Medina, HNRNPA1 regulates HMGCR alternative splicing and modulates cellular cholesterol metabolism, Hum. Mol. Genet. 23 (2014) 319–332.

Figure legends

Fig. 1. Effect of FFAs treatment on the lipid droplets accumulation in HepG2 cells

(A) HepG2 cells were treated with 0.25 mM, 0.5 mM and 1.0 mM of a mix of oleate-palmitate fatty acids (FFAs) in the ratio of 2:1 for the indicated times. Then, cells were harvested and the content of lipid measured in FFAs-treated cells was expressed as percentage relative to the lipid content in untreated control cells. Values are means ± S.D. Within the same group, samples bearing different letters differ significantly (P <0.05, n=5).

(B) Viability of the cells was assessed by MTT assay. Cells were incubated in DMEM medium containing 0.25 mM, 0.5 mM and 1.0 mM FFAs, for the indicated times. Values are means ± S.D. Within the same group, samples bearing different letters differ significantly (P <0.05, n=5).

Fig. 2. FFAs treatment induces the expression of SREBP-1a and of its lipogenic target genes

(A) HepG2 cells were incubated in the presence of 0.5 mM FFAs for the indicated times. Cells were then harvested and total RNA was extracted. SREBP-1a mRNA level was determined by using RT-

qPCR and normalized with 18S rRNA. Values were reported in histograms as fold change relative to the untreated control cells. Values are means ± S.D. Different letters indicate significant differences (P <0.05, n=5).

(B) HepG2 cells were incubated with FFAs as described in Fig. 2A. Proteins (50 μg) were separated by SDS/PAGE and immunoblotted with antisera against SREBP-1a. The content of the precursor (pSREBP-1a) and nuclear (nSREBP-1a) SREBP-1a in FFAs-treated cells was analysed by Western blotting, quantified by densitometric analysis, and was expressed as fold change relative to SREBP-1a content in untreated control cells. Values are means ± S.D. Within the same group, samples bearing different letters differ significantly (P <0.05, n=4).

(**C**) Hep G2 cells, incubated for 12 h in DMEM with either vehicle (BSA) or 0.5 mM FFAs, were then treated with 100 μg/ml cycloheximide, inhibitor of protein synthesis. At different times, cells were harvested and the content of either pSREBP-1 or nSREBP-1 protein was measured by Western blot analysis. The semi-log plot represents the decay curve of pSREBP-1a (squares) or nSREBP-1a (circles) protein in control (filled) and FFAs-treated (open) Hep G2 cells, incubated in the absence (left-hand panel) or in the presence (right-hand panel) of 10 μg/ml cholesterol and 1 μg/ml 25-hydroxycholesterol.

(D) The histograms represent the abundance of CiC, FASN and ACACA mRNA determined using RT-qPCR and expressed as relative amounts (18S rRNA as a reference) in HepG2 treated with FFAs for the indicated times with respect to control. Values were reported in histograms as described in Fig. 2A. Values are means ± S.D. Within the same group, samples bearing different letters differ significantly (P <0.05, n=5).

Fig. 3. FFAs trigger ER-stress and enhance the cap-independent translation of SREBP-1a in HepG2 cells

The upper panel depicts the bicistronic constructs used. pRS1aF, pRc-mycF, and pREF contain the SREBP-1a, c-*myc*, and EMCV IRES regions, respectively. Lower panel, HepG2 cells were co-transfected with a reporter plasmid (pRS1aF, or pRc-mycF, or pREF), and with the control plasmid pCMV-SPORT-β-gal as reported in "Materials and Methods". White and black columns depict *Renilla* (RL) and firefly (FL) luciferase activities, respectively. Luciferase activity measured in untreated transfected cells was set to 1 and values are means ± S.D. Within the same group, samples bearing different letters differ significantly (P <0.05, n=5)

Fig. 4. Effect of FFAs-induced ER stress on the hnRNP A1 expression and on the nucleo-cytosolic shuttling of hnRNP A1

(A) HepG2 cells were treated with 0.5 mM FFAs for the indicated times. Cells were harvested and the nuclear and cytosolic proteins were extracted. The level of hnRNP A1 was determined by Western

blotting analysis and normalized with respect to the Lamin B or to the β-Actin, used as a control for the nuclear and for cytosolic extracts, respectively. Values of normalised level of hnRNP A1 are reported in histograms as means ± S.D. Within the same group, samples bearing different letters differ significantly (P <0.05, n=4).

(B) HepG2 cells were pre-treated with 20 μM MG-132, an inhibitor of ubiquitin-26S proteasome system. After 1 hour, cells were treated with 0.5 mM FFAs and the hnRNP A1 level was determined in nuclear and cytosolic protein extracts as described above. Values of normalised level of hnRNP A1 are reported in histograms as means ± S.D. Within the same group, samples bearing different letters differ significantly (P <0.05, n=4).

(C) HepG2 cells were treated with 0.5 mM FFAs for the indicated times and the abundance of hnRNP A1 mRNA was determined by RT-qPCR and normalized with 18S rRNA. Values of normalised level of hnRNP A1 are reported in histograms as means ± S.D. Different letters indicate significant differences (P < 0.05, n=4).

(D) HepG2 cells were transfected with a plasmid containing the hnRNP A1 promoter inserted upstream the firefly reporter gene. After 24 h, cells were treated with 0.5 mM FFAs for the indicated times and FL activity was measured. Luciferase activity measured in untreated transfected cells was set to 1 and values are means ± S.D. Different letters indicate significant differences (P < 0.05, n=5).

(E) Cytosolic protein extracts were prepared from untreated HepG2 cells (-) or from HepG2 cells treated with 0.5mM FFAs (+) for 6 hours and subjected to an *in vitro* RNA affinity chromatography assay with biotinylated RNA probes corresponding to EMCV or SREBP-1a IRES. Proteins bound to RNA probes were electrophoresed on 12% (w/v) SDS-PAGE and the hnRNP A1 protein level was analysed by Western blotting analysis, by using hnRNP A1 monoclonal antibody. The results are from a representative experiment and similar data were obtained in four independent experiments.

Fig. 5. Involvement of p38 MAPK, Akt and ERK1/2 kinases on the FFAs-mediated induction of SREBP-1a expression

(A) HepG2 cells were treated with 0.5 mM FFAs for the indicated times and protein extracts were separated by 10% SDS-PAGE and analysed by Western-blotting using the antibodies against the active (dually phosphorylated) ERK1/2 (p-ERK), the active p38 MAPK (p-p38 MAPK), the active Akt (p-Akt), and against the total ERK1/2 (ERK), p38 MAPK and Akt. The level of active, phosphorylated form of each kinase was normalized with respect to the corresponding total level. The results are representative of four independent experiments and the data from densitometry are expressed as mean ± S.D. of sum of the grey level values. Within the same group, samples bearing different letters differ significantly (P <0.05, n=4).

(B) HepG2 cells were pre-incubated for 1h with or without 30 μM PD98059 (PD), or 25μM LY294002 (LY), or 10 μM SB203580 (SB), inhibitors of ERK, Akt and p38 MAPK, respectively. Then, cells were treated with or without 0.5 mM FFAs for 6 h. Lysates from HepG2 cells were separated by 10% SDS-PAGE and analysed by Western-blotting using the antibodies against hnRNP A1 (left panel) or SREBP-1a (right panel), and β-Actin (control). Values of normalised levels of precursor (pSREBP-1a) and nuclear (nSREBP-1a) SREBP-1a and hnRNP A1 were reported in histograms as percentage of those obtained in untreated control cells (*C*). Values are means ± S.D. Within the same group, samples bearing different letters differ significantly (P <0.05, n=4).

(C) HepG2 cells were transfected with p38 MAPK siRNA or scramble siRNA. After 48 h, cells were treated with 0.5 mM FFAs for 6 hours and harvested. The levels of cytosolic hnRNP A1 (white column), pSREBP-1a (grey column) and nSREBP-1a (black column) proteins were determined by Western blotting. The normalized level of hnRNP A1, pSREBP-1a, and nSREBP-1a in HepG2 cells transfected with scramble siRNA was set to 1. The results are from a representative experiment and are similar to those obtained in four independent experiments. Within the same group, samples bearing different letters differ significantly (P <0.05, n=4).

Fig. 6. Effect of hnRNP A1 knockdown on the FFAs-mediated induction of SREBP-1a expression in HepG2 cells

(A) HepG2 cells were transfected with hnRNP A1 siRNA or scramble siRNA. After 48 h, cells were transfected with the plasmid expressing hnRNP A1 (pcDNA-hnRNPA1), or the empty vector pcDNA3 for 24 h and then treated with 0.5 mM FFAs for 6 hours and harvested. The levels of pSREBP-1a (white column) and nSREBP-1a (black column) protein were determined by Western blotting. The normalized level of SREBP-1a protein in HepG2 cells transfected with pcDNA empty vector together with the scramble siRNA was set to 1. The results are from a representative experiment and are similar to those obtained in four independent experiments. Within the same group, samples bearing different letters differ significantly (P <0.05, n=4).

(B) HepG2 cells were transfected as described in Fig. 6A. After 48 h, cells were transfected with the pRS1aF for 24 h, treated with 0.5 mM FFAs for 6 hours and then harvested. *Renilla* (RL) and firefly (FL) luciferase activities were determined. Luciferase activity in cells transfected with the empty vector pcDNA3 was set to 1. White and black columns depict RL and FL activities, respectively. Values are means ± S.D. Within the same group, samples bearing different letters differ significantly (P <0.05, n=5)

(C) HepG2 cells were transfected as described in Fig. 6A and the abundance of CiC, FASN and ACACA mRNA was determined using RT-qPCR and expressed as relative amounts (18S rRNA as a reference). The abundance of CiC, FASN and ACACA mRNA was reported in histograms as fold

change with respect to the control cells, co-transfected with pcDNA empty vector together with the scramble siRNA. Values are means ± S.D. Within the same group, samples bearing different letters differ significantly (P <0.05, n=5).

(D) HepG2 cells were transfected as described in Fig. 6A and the lipid accumulation was reported in histograms as fold change with respect to the control cells, as described in Fig. 6C. Values are means ± S.D. Samples bearing different letter differ significantly (P <0.05, n=5).

Fig. 7. Effect of FFAs treatment on the expression of genes for proteins involved in the SREBP-1a proteolytic cleavage

(A) HepG2 cells were treated with 0.5 mM FFAs for the indicated times. Cells were harvested and total proteins and mRNA were extracted. The protein level of SCAP, Insig-1, Insig-2, S1P, S2P, and β-Actin was determined by Western blotting analysis. Values of normalised level of Insig1 and SCAP are reported in histograms as means ± S.D. Within the same group, samples bearing different letters differ significantly (P <0.05, n=4).

(B) The abundance of Insig-1, Insig-2, SCAP, S1P, and S2P mRNA was determined using RT-qPCR, expressed as relative amounts (18S rRNA as a reference), and reported in histograms as fold change with respect to the untreated control cells (Time 0).

Supplementary Fig. 1. BSA treatment did not induce the expression of SREBP-1a

(A) HepG2 cells were incubated in the presence of 0.125 mM BSA for the indicated times. Cells were then harvested and total RNA was extracted. SREBP-1a mRNA level was determined by using RT-qPCR and normalized with 18S rRNA. Values were reported in histograms as fold change relative to the untreated control cells. Values are means ± S.D. Different letters indicate significant differences (P < 0.05, n=5).

(B) HepG2 cells were incubated with BSA as described in Fig. 2A. Proteins (50 μg) were separated by SDS/PAGE and immunoblotted with antisera against SREBP-1a. The content of the precursor (pSREBP-1a) and nuclear (nSREBP-1a) SREBP-1a in FFAs-treated cells was analysed by Western blotting, quantified by densitometric analysis and was expressed as fold change relative to SREBP-1 content in cells cultured in untreated control cells. Values are means ± S.D. Within the same group, samples bearing different letters differ significantly (P <0.05, n=4).

Supplementary Fig. 2. FFAs trigger ER-stress in HepG2 cells

HepG2 cells were incubated in the presence of 0.5 mM FFAs for the indicated times. Total protein extracts (50 μg) were fractionated by 10% SDS-PAGE and immunodecorated with the antibody against GRP78. β-Actin was used as a control. Nuclear protein extracts (50 μg) were fractionated as above and immunodecorated with the antibody against XBP1. Lamin B was used as a control. The content of GRP78 and XBP1 in FFAs-treated cells was quantified by densitometric analysis and

expressed as fold change with respect to untreated control cells. Values are means ± S.D., *n*=4. Within the same group, samples bearing different letters differ significantly.

Figure 1

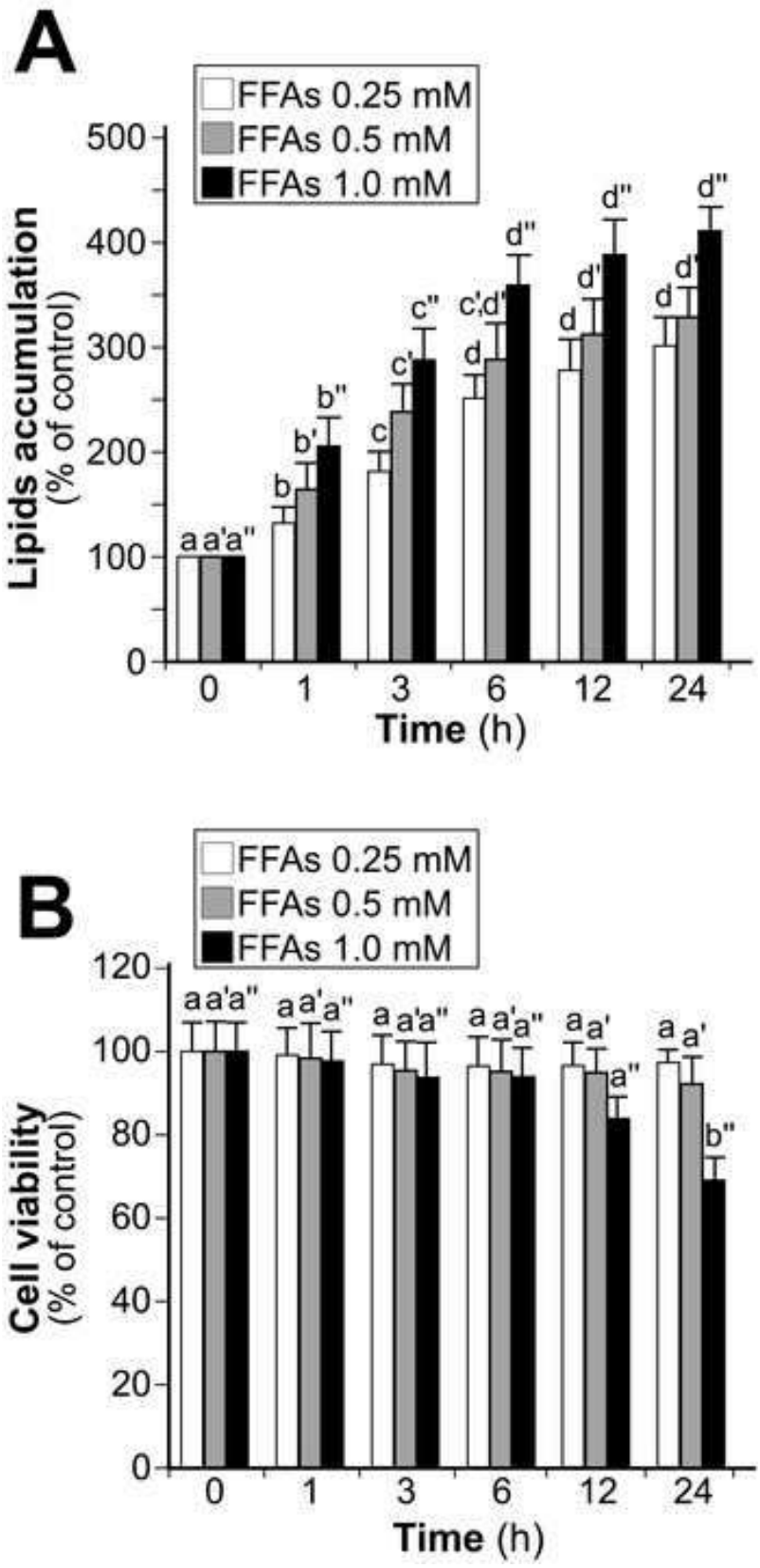
A
FFAs 0.25 mM
FFAs 0.5 mM
FFAs 1.0 mM
Lipids accumulation
(% of control)
500
400
300
200
100
0
a a'a"
b
b'
b"
c
c'
c"
c'd'
d
d"
d
d'
d"
d
d'
d"
0
1
3
6
12
24
Time (h)
B
FFAs 0.25 mM
FFAs 0.5 mM
FFAs 1.0 mM
Cell viability
(% of control)
120
100
80
60
40
20
0
a a'a"
a a'a"
a a'a"
a a'a"
a a'
a"
a a'
b"
0
1
3
6
12
24
Time (h)

Figure 2

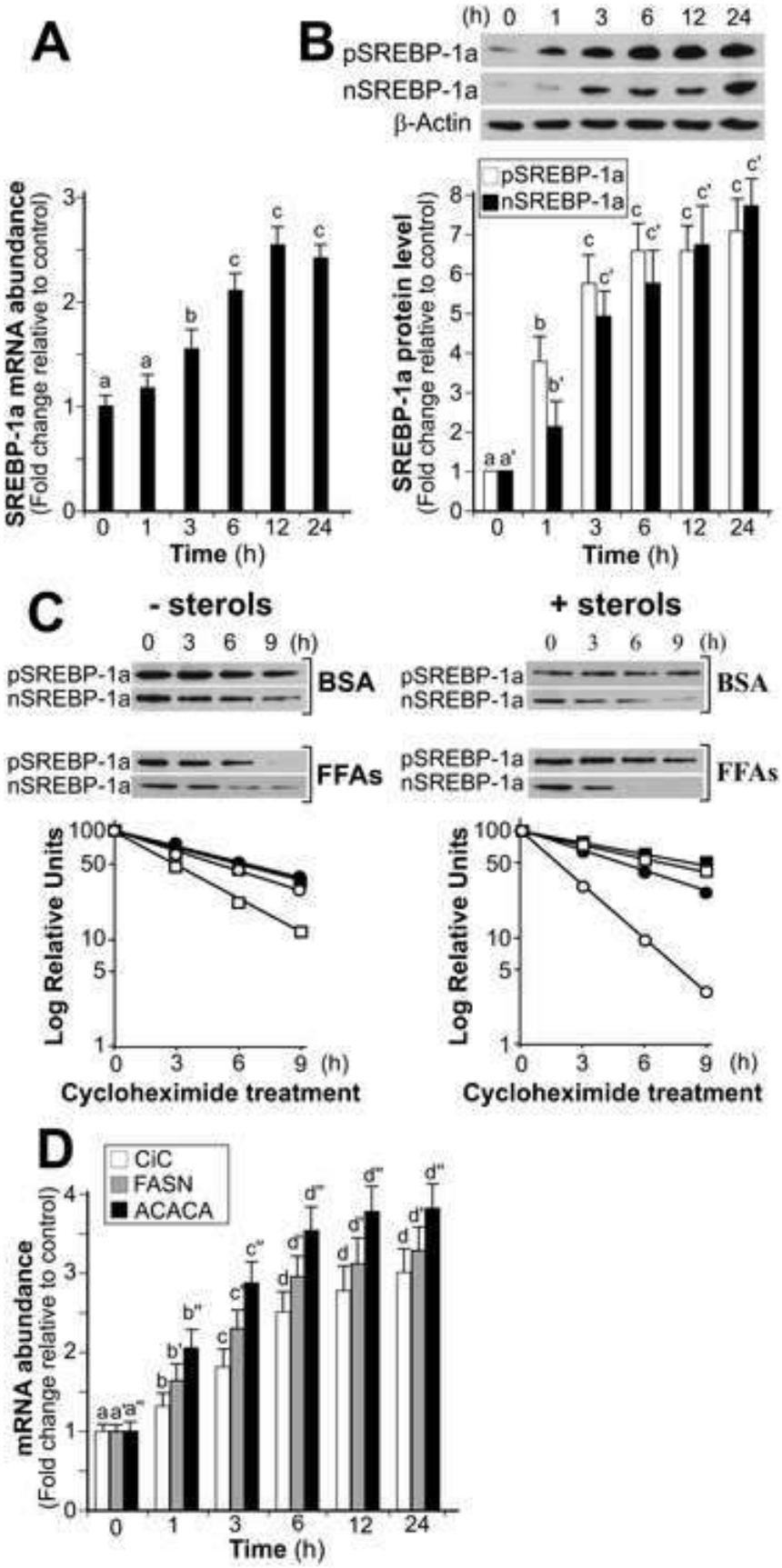
A
B
(h) 0 1 3 6 12 24
pSREBP-1a
nSREBP-1a
β-Actin
SREBP-1a mRNA abundance
(Fold change relative to control)
Time (h)
pSREBP-1a
nSREBP-1a
SREBP-1a protein level
(Fold change relative to control)
Time (h)
C
- sterols
+ sterols
0 3 6 9 (h)
pSREBP-1a
nSREBP-1a
BSA
FFAs
Log Relative Units
Cycloheximide treatment
D
CiC
FASN
ACACA
mRNA abundance
(Fold change relative to control)
Time (h)

Figure 3

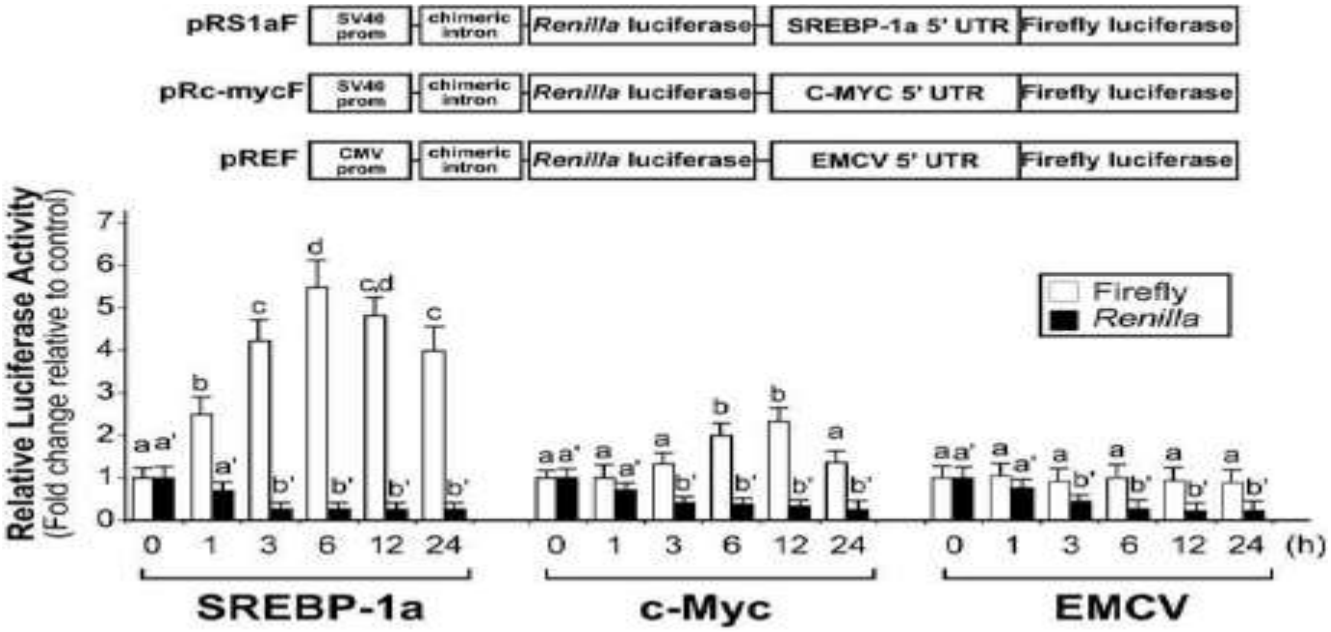
pRS1aF
SV40 prom
chimeric intron
Renilla luciferase
SREBP-1a 5' UTR
Firefly luciferase
pRc-mycF
SV40 prom
chimeric intron
Renilla luciferase
C-MYC 5' UTR
Firefly luciferase
pREF
CMV prom
chimeric intron
Renilla luciferase
EMCV 5' UTR
Firefly luciferase
Relative Luciferase Activity
(Fold change relative to control)
Firefly
Renilla
0 1 3 6 12 24 (h)
SREBP-1a
c-Myc
EMCV

Figure 4

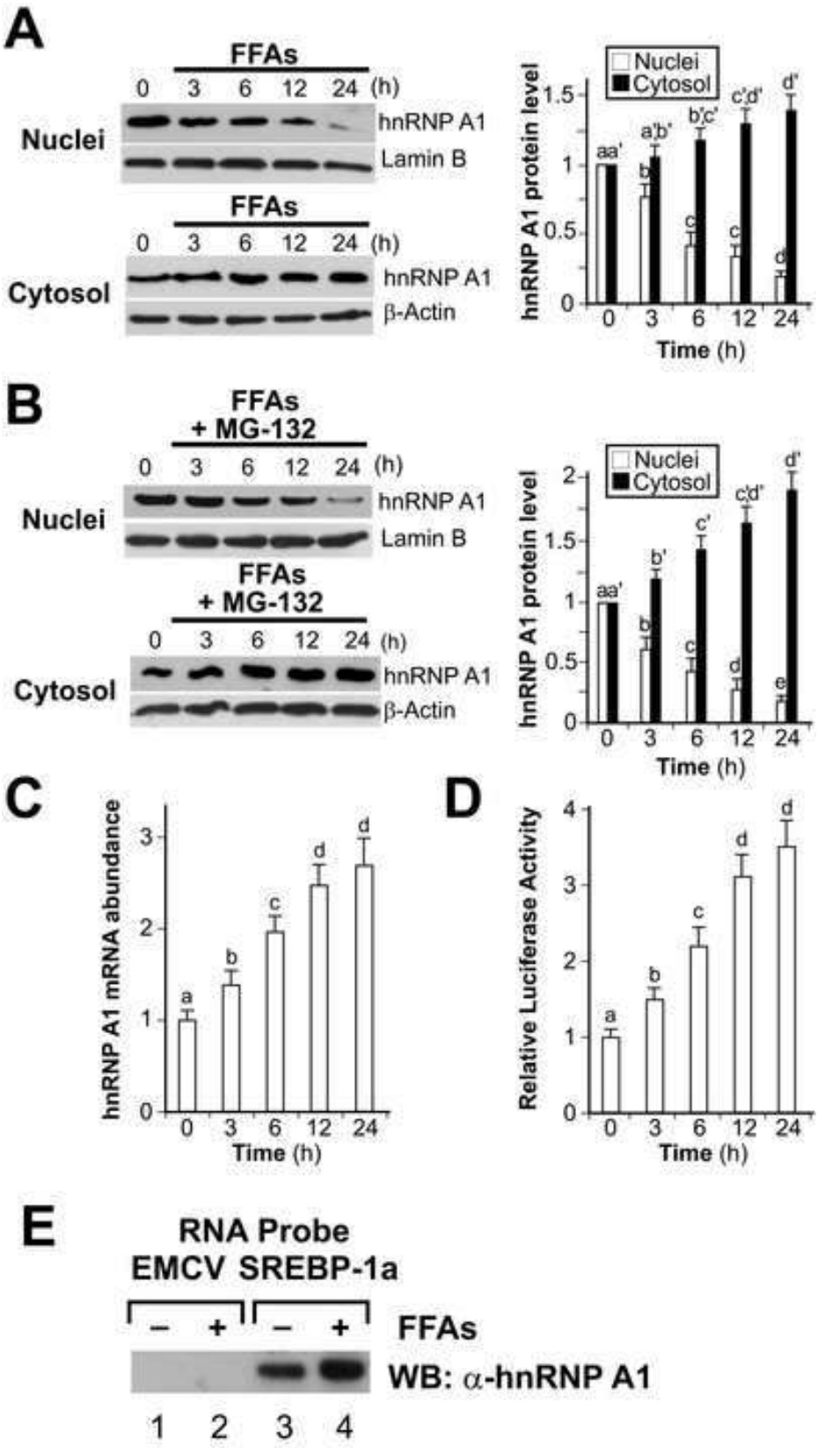
A
FFAs
0 3 6 12 24 (h)
Nuclei
hnRNP A1
Lamin B
FFAs
0 3 6 12 24 (h)
Cytosol
hnRNP A1
β-Actin
Nuclei
Cytosol
hnRNP A1 protein level
Time (h)
B
FFAs
+ MG-132
0 3 6 12 24 (h)
Nuclei
hnRNP A1
Lamin B
FFAs
+ MG-132
0 3 6 12 24 (h)
Cytosol
hnRNP A1
β-Actin
Nuclei
Cytosol
hnRNP A1 protein level
Time (h)
C
hnRNP A1 mRNA abundance
Time (h)
D
Relative Luciferase Activity
Time (h)
E
RNA Probe
EMCV SREBP-1a
– + – +
FFAs
WB: α-hnRNP A1
1 2 3 4

Figure 5

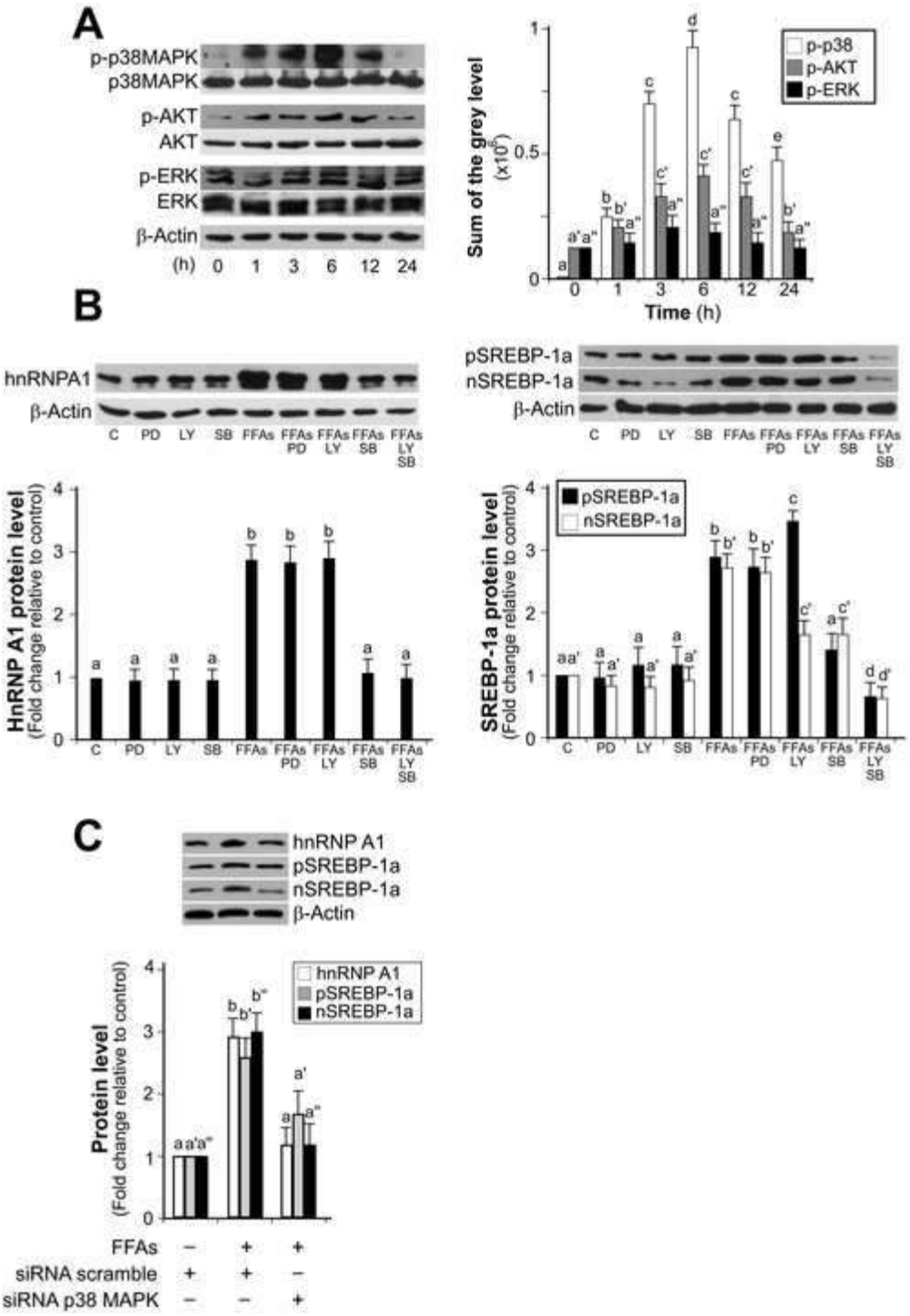
A
p-p38MAPK
p38MAPK
p-AKT
AKT
p-ERK
ERK
β-Actin
(h) 0 1 3 6 12 24
Sum of the grey level (x10⁶)
Time (h)
p-p38
p-AKT
p-ERK
B
hnRNPA1
β-Actin
pSREBP-1a
nSREBP-1a
C PD LY SB FFAs FFAs PD FFAs LY FFAs SB FFAs LY SB
HnRNP A1 protein level (Fold change relative to control)
SREBP-1a protein level (Fold change relative to control)
C
hnRNP A1
pSREBP-1a
nSREBP-1a
β-Actin
Protein level (Fold change relative to control)
FFAs
siRNA scramble
siRNA p38 MAPK

Figure 6

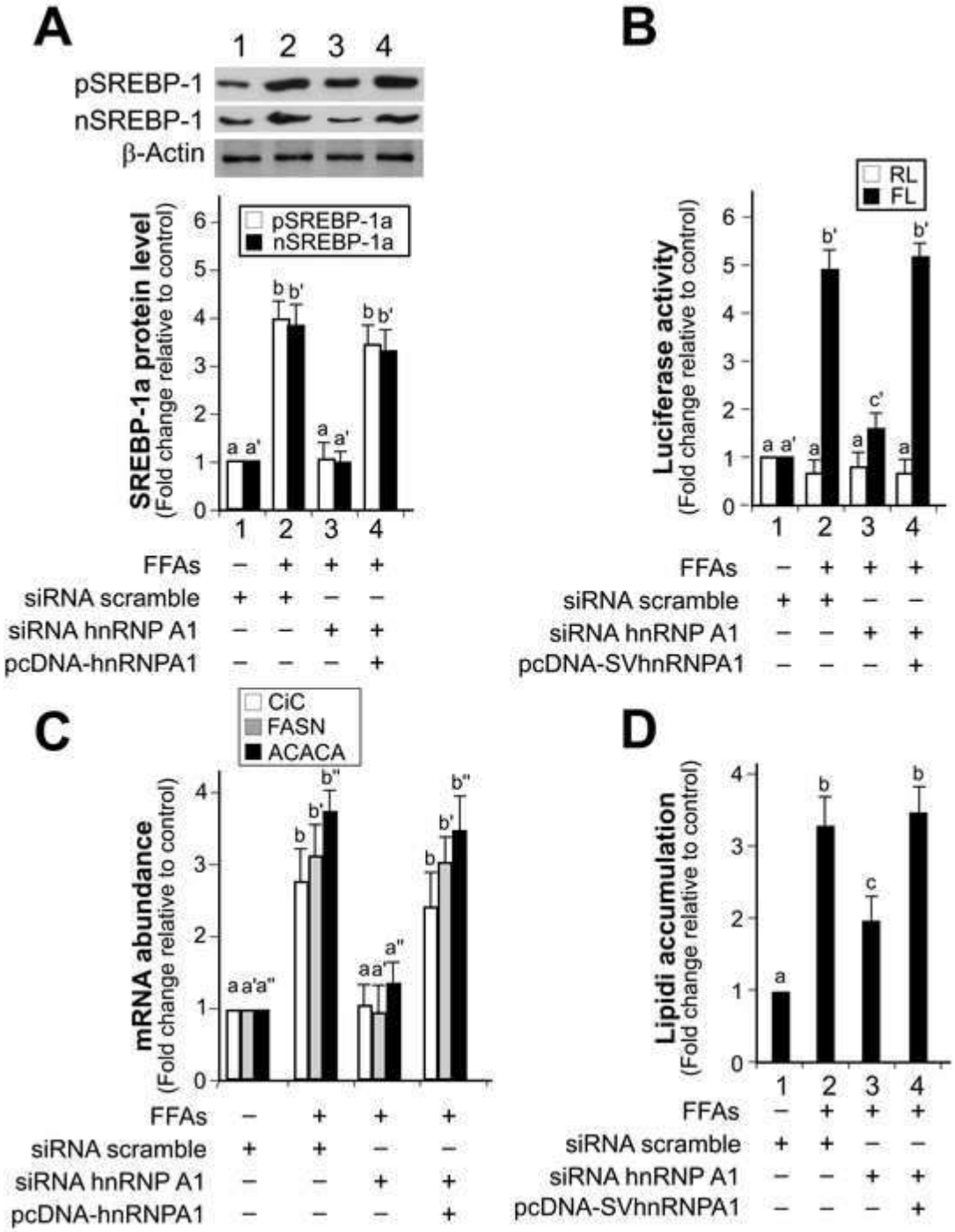
A
1 2 3 4
pSREBP-1
nSREBP-1
β-Actin
SREBP-1a protein level
(Fold change relative to control)
pSREBP-1a
nSREBP-1a
FFAs
siRNA scramble
siRNA hnRNP A1
pcDNA-hnRNPA1
B
Luciferase activity
(Fold change relative to control)
RL
FL
FFAs
siRNA scramble
siRNA hnRNP A1
pcDNA-SVhnRNPA1
C
CiC
FASN
ACACA
mRNA abundance
(Fold change relative to control)
FFAs
siRNA scramble
siRNA hnRNP A1
pcDNA-hnRNPA1
D
Lipidi accumulation
(Fold change relative to control)
FFAs
siRNA scramble
siRNA hnRNP A1
pcDNA-SVhnRNPA1

Figure 7

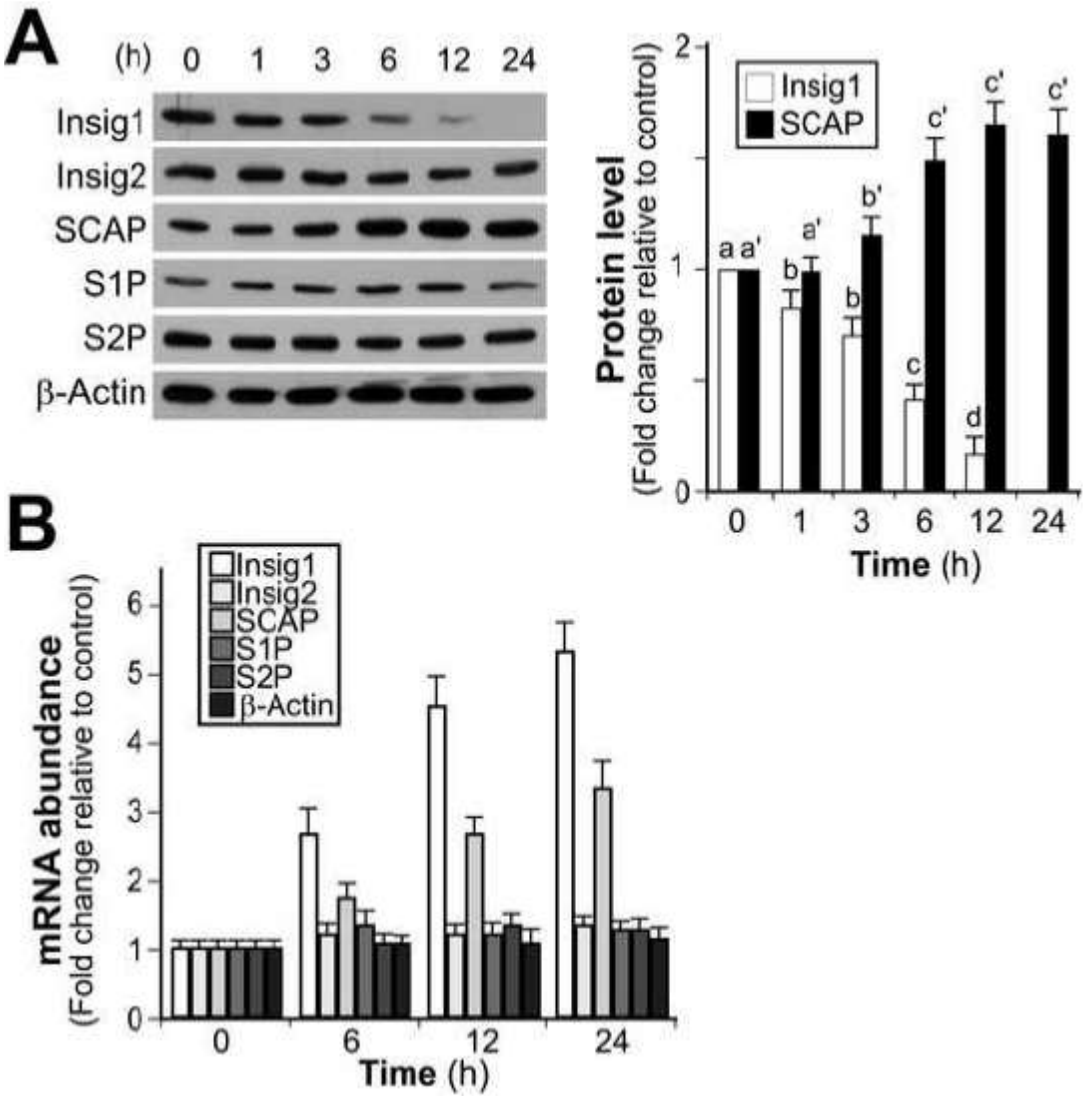
A
(h) 0 1 3 6 12 24
Insig1
Insig2
SCAP
S1P
S2P
β-Actin
Protein level
(Fold change relative to control)
Insig1
SCAP
a a'
b a'
b b'
c c'
d c'
c'
0 1 2
0 1 3 6 12 24
Time (h)
B
mRNA abundance
(Fold change relative to control)
Insig1
Insig2
SCAP
S1P
S2P
β-Actin
0 1 2 3 4 5 6
0 6 12 24
Time (h)

Supplementary Figure 1

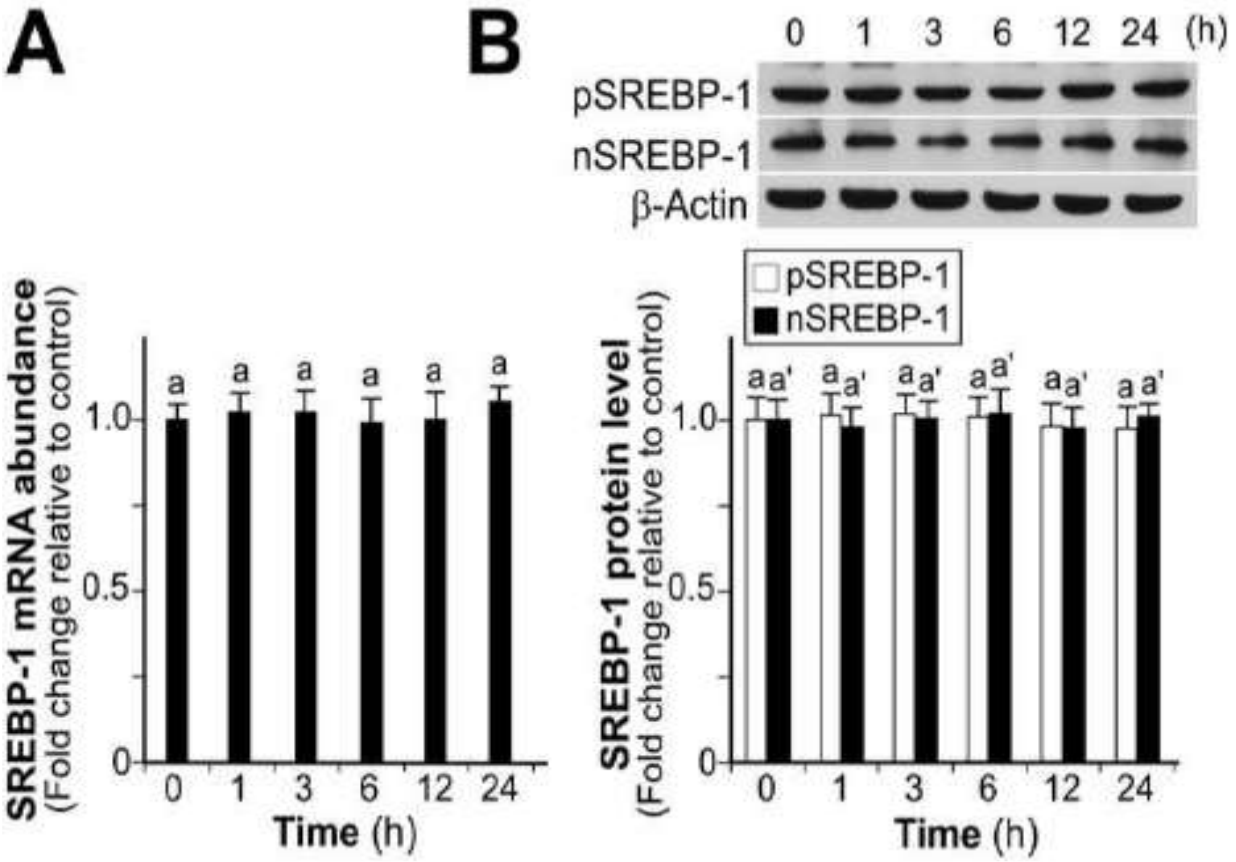

Supplementary Figure 2